Marquette University
e-Publications@Marquette

Biological Sciences Faculty Research and Publications

Biological Sciences, Department of

9-1-2018

Effects of Elevated H⁺ And P$_i$ on The Contractile Mechanics of Skeletal Muscle Fibres From Young and Old Men: Implications for Muscle Fatigue in Humans

Christopher W. Sundberg
Marquette University

Sandra K. Hunter
Marquette University, sandra.hunter@marquette.edu

Todd A. Trappe
Ball State University

Carolyn S. Smith
Marquette University, carolyn.s.smith@marquette.edu

Robert H. Fitts
Marquette University, robert.fitts@marquette.edu

Biology Faculty Research and Publications/College of Arts and Sciences

Effects of Elevated H+ And Pi on The Contractile Mechanics of Skeletal Muscle Fibres From Young and Old Men: Implications for Muscle Fatigue in Humans

Christopher W. Sundberg
Exercise Science Program, Marquette University, Milwaukee, WI
Clinical & Translational Rehabilitation Health Sciences Program, Department of Physical Therapy, Marquette University, Milwaukee, WI

Sandra K. Hunter
Exercise Science Program, Marquette University, Milwaukee, WI
Clinical & Translational Rehabilitation Health Sciences Program, Department of Physical Therapy, Marquette University, Milwaukee, WI

Scott W. Trappe

Human Performance Laboratory, Ball State University, Muncie, IN

Carolyn S. Smith

Exercise Science Program, Marquette University, Milwaukee, WI

Robert H. Fitts

Department of Biological Sciences, Marquette University, Milwaukee, WI

Key points

- The mechanisms responsible for the loss in muscle power and increased fatigability with ageing are unresolved.
- We show that the contractile mechanics of fibres from the vastus lateralis of old men were well-preserved compared to those of young men, but the selective loss of fast myosin heavy chain II muscle was strongly associated with age-related decrements in whole-muscle strength and power.
- We reveal that the combination of acidosis (H^+) and inorganic phosphate (P_i) is an important mediator of muscle fatigue in humans by inhibiting the low- to high-force state of the cross-bridge cycle and peak power, but the depressive effects of these ions on cross-bridge function were similar in fibres from young and old men.
- These findings suggest that the age-related loss in muscle power is primarily determined by the atrophy of fast fibres, but the age-related increased fatigability cannot be explained by an increased sensitivity of the cross-bridge to H^+ and P_i.

Abstract

The present study aimed to identify the mechanisms responsible for the loss in muscle power and increased fatigability with ageing by integrating measures of whole-muscle function with single fibre contractile mechanics. After adjusting for the 22% smaller muscle mass in old (73–89 years, $n = 6$) compared to young men (20–29 years, $n = 6$), isometric torque and power output of the knee extensors were, respectively, 38% and 53% lower with age. Fatigability was ~2.7-fold greater with age and strongly associated with reductions in the electrically-evoked contractile properties. To test whether cross-bridge mechanisms could explain age-related decrements in knee extensor function, we exposed myofibres ($n = 254$) from the vastus lateralis to conditions mimicking quiescent muscle and fatiguing levels of acidosis (H^+) (pH 6.2) and inorganic phosphate (P_i) (30 mM). The fatigue-mimicking condition caused marked reductions in force, shortening velocity and power and inhibited the low- to high-force state of the cross-bridge cycle, confirming findings from non-human studies that these ions act synergistically to impair cross-bridge function. Other than severe age-related atrophy of fast fibres (−55%), contractile function and the depressive effects of the fatigue-mimicking condition did not differ in fibres from young and old men. The selective loss of fast myosin heavy chain II muscle was strongly associated with the age-related decrease in isometric torque ($r = 0.785$) and power ($r = 0.861$). These data suggest that the age-related loss in muscle strength and power are primarily determined by the atrophy of fast fibres, but the age-related increased fatigability cannot be explained by an increased sensitivity of the cross-bridge to H^+ and P_i.

Introduction

Human ageing is accompanied by a progressive decline in neuromuscular function, which acts to reduce mobility, increase the risk of falling and limit the performance of daily activities in older adults. Pivotal for the

age-related decline in function is the loss in muscle mass that can approach 30% in individuals ≥60 years of age (Doherty, **2003**). However, the age-related losses in maximal strength and the ability to generate power occur earlier in life and at a more rapid rate than the losses in total muscle mass, suggesting that other factors such as changes in the nervous system and 'muscle quality' also contribute to the losses in function with age (Reid & Fielding, **2012**; Russ *et al*. **2012**; Hepple & Rice, **2016**; Hunter *et al*. **2016**). Additionally, the age-related decline in the ability to generate power is exacerbated by the increase in fatigability that occurs when older adults perform moderate- to high-velocity contractions (McNeil & Rice, **2007**; Dalton *et al*. **2010**; Callahan & Kent-Braun, **2011**; Dalton *et al*. **2012**). Despite the growing recognition that muscle power output is an important predictor of functional impairments in older adults (Reid & Fielding, **2012**), the primary mechanisms for the loss in mechanical power and the increase in fatigability with ageing remain unresolved.

Fatigability of limb muscle, often termed fatigue or muscle fatigue, is characterized by an acute reduction in force and power in response to contractile activity and can occur as a result of changes anywhere along the motor pathway (Kent-Braun *et al*. **2012**; Hunter, **2017**). Studies from the intact neuromuscular system of older adults report that the mechanisms for the age-related increase in fatigability during dynamic exercise are primarily a result of factors within the muscle (Baudry *et al*. **2007**; Dalton *et al*. **2010**, **2012**). More specifically, we recently showed that the age-related increase in power loss during a dynamic knee extension exercise was strongly associated with reductions in both the amplitude and rate of torque development of the electrically-evoked twitch (Sundberg *et al*. **2018**). The latter is believed to be limited by the forward rate constant of the low- to high-force state of the cross-bridge cycle, suggesting that the mechanism responsible for the age-related increase in fatigability during dynamic exercise is a result of cellular mechanisms that disrupt cross-bridge function (Fitts, **1994**, **2008**).

In isolated permeabilized muscle fibres, the kinetics of the low- to high-force state of the cross-bridge cycle can be measured by employing a rapid slack re-extension manoeuvre of a maximally Ca^{2+}-activated fibre (Metzger & Moss, **1990a**,*b*). The rapid re-extension of the fibre dissociates myosin from actin and the rate of force redevelopment (k_{tr}) following the re-extension represents the sum of the forward and reverse rate constants of the low- to high-force state of the cross-bridge cycle (Brenner & Eisenberg, **1986**; Metzger *et al*. **1989**). Two metabolic by-products implicated in fatigue, inorganic phosphate (P_i) and hydrogen (H^+), have been shown to directly affect the cross-bridge cycle at this transition step, but by different mechanisms (Debold *et al*. **2016**). Specifically, P_i is believed to induce an unconventional powerstroke where myosin dissociates from actin early in the low- to high-force transition (Linari *et al*. **2010**; Caremani *et al*. **2013**; Debold *et al*. **2016**), resulting in the acceleration of the rate of force development (Dantzig *et al*. **1992**) and k_{tr} (Wahr *et al*. **1997**; Tesi *et al*. **2002**). By contrast, H^+ is believed to inhibit the forward rate constant of the low- to high-force state (Metzger & Moss, **1990b**), which may explain the lack of difference in k_{tr} in rat fibres exposed to a control (pH 7.0 + 0 mM P_i) compared to a combined P_i (30 mM) and H^+ (pH 6.2) condition (Nelson *et al*. **2014**). However, because the resting concentration of P_i in quiescent human skeletal muscle is ∼3-5 mM (Kemp *et al*. **2007**), these previous studies may have underestimated the effect of H^+ on k_{tr}. In addition, no studies have tested the effects of P_i and H^+ on human skeletal muscle and only a single study has measured k_{tr} of 'slow type' fibres from old compared to young adults (Power *et al*. **2016**). Thus, the first aim of the present study was to compare the k_{tr} of fibres expressing slow myosin heavy chain (MHC) I and fast MHC II from young (<30 years) and old adults (>70 years) in conditions mimicking quiescent human muscle (pH 7.0 + 4 mM P_i) and severe fatigue (pH 6.2 + 30 mM P_i). We hypothesized that the k_{tr} of both fibre types would be lower in the fibres from old compared to young adults,

and that the fatigue-mimicking condition would slow k_{tr} but would do so to a greater extent in the fibres from old adults.

In addition to the experiments on the low- to high-force transition of the cross-bridge cycle, experiments on peak isometric force (P_o), shortening velocity (V_o and V_{max}) and peak fibre power are necessary to assess whether cross-bridge mechanisms are responsible for the age-related loss in power and increase in fatigability. When studied in isolation at cold temperatures (<20°C), both P_i and H^+ cause large reductions in P_o and peak fibre power, whereas H^+ alone also slows shortening velocity (Metzger & Moss, **1987**; Chase & Kushmerick, **1988**; Cooke *et al*. **1988**; Godt & Nosek, **1989**; Debold *et al*. **2004**; Knuth *et al*. **2006**). Subsequent studies performed at near physiological temperatures (30°C) have generally found a reduced effect of P_i and H^+ on P_o and peak power, but that the effect of H^+ on shortening velocity was unaltered by temperature (Debold *et al*. **2004**; Knuth *et al*. **2006**; Karatzaferi *et al*. **2008**). The mitigated effect of these ions at near *in vivo* temperatures has lead to considerable debate over their role in the fatigue process (Fitts, **2016**; Westerblad, **2016**). However, when the effects of elevated H^+ (pH 6.2) and P_i (30 mM) were studied in combination at 30°C, which is more relevant to the fatigue process *in vivo*, they had a synergistic effect that caused marked reductions in P_o ($\sim$35–50%), peak power ($\sim$55–65%) and V_{max} ($\sim$20%) of rat and rabbit fibres (Karatzaferi *et al*. **2008**; Nelson *et al*. **2014**).

Therefore, the second aim of the present study was to test the effects of the fatigue-mimicking condition (pH 6.2 + 30 mM P_i) on P_o, V_o and V_{max}, and peak power in fibres from young and old adults at 15 and 30°C. We hypothesized that the age-related increase in fatigability during dynamic exercise is due, in part, to an increased sensitivity of the cross-bridge of old adult fibres to H^+ and P_i. Importantly, because we integrated measures of whole-muscle function with single cell contractile mechanics, the third aim of the present study was to explore the mechanisms for the age-related loss in 'muscle quality' (i.e. decreased strength or power after normalizing for differences in muscle mass, volume or cross-sectional area).

Methods

Participants and ethical approval

Six young men (20–29 years) and six old men (73–89 years) volunteered and provided their written informed consent to participate in the present study. Participants underwent a general health screening and were excluded from the study if they were taking medications that affect the central nervous system, muscle mass or neuromuscular function (e.g. hormone-replacement therapies, anti-depressants, glucocorticoids). All participants were apparently healthy, community dwelling adults free of any known neurological, musculoskeletal or cardiovascular diseases. All experimental procedures were approved by the Marquette University Institutional Review Board and conformed to the principles in the *Declaration of Helsinki*.

Physical activity (PA) assessment

PA was quantified for each participant with a triaxial accelerometer (GT3X; ActiGraph, Pensacola, FL, USA) worn around the waist for at least 4 days (2 weekdays and 2 weekend days) as reported previously (Hassanlouei *et al*. **2017**). The data were reported for each participant as long as the participant completed at least 3 days of wear time (Hart *et al*. **2011**).

Whole-muscle knee extensor function and fatigability

Participants reported to the laboratory on four occasions: twice for familiarization, once for an experimental session to measure whole-muscle function of the knee extensors and once for a muscle biopsy of the vastus lateralis. The familiarization sessions were used to habituate the participants to electrical stimulation of the femoral nerve and transcranial magnetic stimulation (TMS) to the motor cortex. Participants also practiced performing maximal voluntary isometric and concentric contractions with the knee extensors during the familiarization sessions. The experimental session assessed whether old adults demonstrated conventional age-related changes of the knee extensor muscles compared to young adults, including (i) lower thigh lean muscle mass; (ii) lower absolute and mass-specific isometric strength and mechanical power outputs; and (iii) an increased fatigability (reductions in mechanical power) when performing a high-velocity dynamic exercise (Dalton *et al*. **2012**; Reid & Fielding, **2012**). Results for the fatigability measurements are a subset of the data reported by **Sundberg *et al*. (2018)**.

Thigh lean mass

Body composition and thigh lean mass was assessed by dual X-ray absorptiometry (Lunar iDXA; GE, Madison, WI, USA). Thigh lean mass was quantified for the region of interest using the manufacturer's software (enCORE, version 14.10.022; GE), with the distal demarcation set at the tibiofemoral joint and the proximal demarcation set as a diagonal bifurcation through the femoral neck. DXA measures of thigh lean mass with these landmarks are strongly correlated with measures from magnetic resonance imaging but underestimate the age-related loss in thigh muscle mass (Maden-Wilkinson *et al*. **2013**).

Experimental session

The experimental set-up to measure whole-muscle function of the knee extensors was identical to that described previously (Sundberg *et al*. **2018**). Briefly, testing was performed on the dominant leg of each participant (preferred kicking leg), and participants were seated upright in the high Fowler's position with the starting knee position set at 90° flexion in a Biodex System 4 Dynamometer (Biodex Medical, Shirley, NY, USA). Extraneous movements and changes in hip angle were minimized by securing the participants to the seat with the dynamometer's four-point restraint system. To ensure the measured torques and velocities were generated primarily by the knee extensor muscles, participants were prohibited from grasping the dynamometer with their hands.

Electromyography (EMG)

Surface Ag/AgCl EMG electrodes (Grass Products; Natus Neurology, Warwich, RI, USA) were adhered to the skin in a bipolar arrangement overlying the muscle bellies of the vastus lateralis, vastus medialis, rectus femoris and biceps femoris with an inter-electrode distance of 2.5 cm. The reference electrodes were placed on the patella, and analogue EMG signals were amplified (100×), filtered (13–1000 Hz band pass; Coulbourn Instruments, Allentown, PA, USA), digitized at 2000 Hz and stored online using Spike 2 software (Cambridge Electronics Design, Cambridge, UK).

Electrical stimulation

The experimental session began with electrical stimulation of the femoral nerve to identify the electrode placement that elicited the maximum peak-to-peak compound muscle action potential (maximum M-wave: M_{max}) of the vastus lateralis, rectus femoris and vastus medialis. The femoral nerve was stimulated with a constant-current, variable high-voltage stimulator (DS7AH; Digitimer, Welwyn Garden City, Hertforshire, UK),

with the cathode placed over the nerve high in the femoral triangle and the anode placed over the greater trochanter. Single 200 μs square-wave pulses were delivered with a stimulus intensity beginning at 50 mA and increased incrementally by 50–100 mA until both the unpotentiated resting twitch torque amplitude and M_{max} for all three quadriceps muscles no longer increased. The intensity was then increased by an additional 20% to ensure that the stimuli were supramaximal.

Maximal voluntary contraction (MVC) torque and voluntary activation

Following the electrical stimulations, participants performed a minimum of three brief (2–3 s) knee extension MVCs without stimulation interspersed with at least 60 s of rest. Participants were provided strong verbal encouragement and visual feedback on their performance with a 56 cm monitor mounted 1–1.5 m directly in front of their line of vision. The torque during each MVC was quantified as the average over a 0.5 s interval centered on the peak torque, and MVC attempts were continued until the two highest values were within 5% of each other.

Following the MVCs, the motor cortex was stimulated by delivering a 1 ms duration magnetic pulse with a concave double-cone coil (diameter 110 mm; maximum output 1.4 T) connected to a monophasic magnetic stimulator (Magstim 200^2; Magstim, Whitland, UK). Identification of the optimal stimulator position was guided by moving along a 1 cm grid drawn on an electroencephalography cap and was determined as the location that elicited the greatest motor evoked potential in the vastus lateralis while the subject contracted at 20% MVC. Once the optimal stimulator position was determined, the stimulator intensity for the voluntary activation measurements was identified during brief (2–4 s) isometric contractions at 40% MVC. Single pulse TMS was delivered during each contraction with an intensity starting at 50% stimulator output and increased incrementally until the largest vastus lateralis peak-to-peak motor evoked potential amplitude was achieved.

After the optimal TMS position and intensity were identified, participants performed five sets of brief isometric contractions (2–3 s) coupled with stimulations to obtain the baseline measures used for identifying the sites of fatigue along the motor pathway. Each set of isometric contractions included a MVC followed by contractions at 60% and 80% MVC (MVC-60–80%). Sets were interspersed with at least 2.5 min of rest to ensure repeatable maximal efforts were performed by minimizing the residual fatigue from each set. The highest torque output from all MVC attempts was used to calculate the 20% MVC load for the dynamic fatiguing exercise. To measure voluntary activation during each set, single pulse TMS was delivered during the MVC, 60% and 80% MVC contractions, and the amplitude of the superimposed twitch torque measured for each contraction (Todd *et al*. **2003**; Hunter *et al*. **2006**; Sidhu *et al*. **2009**). A linear regression was performed between the superimposed twitch torque and the voluntary torque to obtain an estimated resting twitch. The resting twitch evoked by TMS was estimated rather than measured directly because resting twitches cannot be elicited by TMS to the motor cortex. Any regression with an $r^2 < 0.8$ was excluded from the voluntary activation calculations with eqn **1**. For comparison of these data with all other studies that have used TMS to assess voluntary activation, we quantified the voluntary activation for each set of MVC-60–80% contractions in two ways:

$$\text{Voluntary activation (\%)} = \left(1 - \frac{\text{SIT}}{\text{eRT}} \right) \times 100$$

$$\text{Voluntary activation (\%)} = \left(1 - \frac{\text{SIT}}{\text{eRT}} \right) \times 100 \tag{1}$$

$$\text{Voluntary activation (\%)} = \left(\frac{\text{SIT}}{\text{SIT} + \text{MVC}}\right) \times 100$$

$$\text{Voluntary activation (\%)} = \left(1 - \frac{\text{SIT}}{\text{SIT+MVC}}\right) \times 100 \quad (2)$$

where SIT is the amplitude of the superimposed twitch torque elicited by TMS during the MVC, and eRT is the estimated resting twitch torque. The baseline voluntary activation for each participant was the median from the five sets of MVC-60–80% contractions performed prior to the dynamic exercise.

Electrically-evoked contractile properties and M-wave

Contractile properties of the knee extensors were quantified with the potentiated resting twitches from the single-pulse femoral nerve stimulations delivered immediately after (<5 s) the MVC and 80% MVC contractions. The baseline values for each participant were the median obtained from the five sets of MVC-60–80% performed prior to the dynamic fatiguing exercise and were reported for the amplitude of the potentiated resting twitch torque (Q_{tw}: Nm), the half-relaxation time (ms) and the peak rate of torque development (Nm s^{-1}). The peak rate of torque development (dT/dt) was quantified with the derivative of the torque channel as the highest rate of torque increase over a 10 ms interval. To provide an indication of neuromuscular propagation and the ability of the action potential to propagate across the sarcolemma, the peak-to-peak amplitude (M_{max}) and area of the M-wave were reported for the vastus lateralis muscle (Fuglevand et al. **1993**).

Dynamic fatiguing exercise

Following the baseline isometric MVC measurements, participants were habituated to performing maximal velocity knee extensions against a 20% MVC load applied by the dynamometer. To minimize the effect of the additional braking force applied by the dynamometer at the end of the range of motion, the maximum total displacement was set to 95° with the starting position at 90° knee flexion. For the dynamic fatiguing exercise, participants were provided strong verbal encouragement to kick as fast as possible once every 3 s for a total of 4 min (80 contractions). Contraction-by-contraction power outputs (W) were calculated as the product of the measured torque (Nm) and angular velocity (rad s^{-1}) and averaged over the entire shortening phase of the knee extension. Because power output increased over the first few contractions in some participants, the baseline power output for each participant was the highest average obtained from five sequential contractions within the first 10 contractions. Fatigability was quantified by expressing the average power output from the last five contractions as a percentage of the individual-specific baseline power output.

Sites of fatigue

To identify the sites of fatigue in the young and old adults, a set of MVC-60–80% contractions was performed as rapidly as possible following the fatiguing exercise (10.1 ± 2.8 s). Changes in voluntary activation with TMS following the dynamic exercise were used to test whether suboptimal neural drive from the motor cortex was contributing to fatigue in either age group (Todd et al. **2003**). To assess whether impaired neuromuscular propagation was contributing to fatigue, changes in the vastus lateralis M-wave area and amplitude were quantified following the exercise (Fuglevand et al. **1993**). Lastly, to test whether disruptions in cross-bridge function and/or excitation contraction coupling were contributing to fatigue, we measured the changes in the electrically-evoked twitch contractile properties (Kent-Braun et al. **2012**).

Muscle biopsy

A muscle biopsy from the vastus lateralis of the leg tested in the whole-muscle experiments was obtained from each participant (Bergstrom, **1962**). Participants were instructed to refrain from strenuous exercise of the lower limb for 48 h prior to the biopsy and arrived at the laboratory fasted and without consumption of caffeine. The biopsy location was cleaned with 70% ethanol, sterilized with 10% providone-iodine and anaesthetized with 1% lidocaine HCl. A small ~1 cm incision was made overlying the distal one-third of the muscle belly, and the biopsy needle was inserted under local suction to obtain the tissue sample. Two longitudinal bundles from the biopsy sample were immediately submerged in cold glycerol skinning solution (see below) and stored at –20°C. The remaining biopsy sample was immediately frozen in liquid nitrogen and stored at –80°C. All single fibre contractile experiments were completed within 4 weeks of the biopsy.

Single fibre morphology and contractile mechanics

Solutions

The composition of the relaxing (pCa 9.0, where pCa = $-\log[Ca^{2+}]$) and activating (pCa 4.5) solutions were derived from an iterative program using the stability constants adjusted for temperature, pH and ionic strength (Fabiato & Fabiato, **1979**; Fabiato, **1988**). All solutions contained (in mM) 20 imidazole, 7 EGTA, 4 MgATP and 14.5 creatine phosphate. Inorganic phosphate (P_i) was added as K_2HPO_4 to yield a concentration of 4 or 30 mM. Although no P_i was added to the 0 mM P_i solution, there is evidence that the actual concentration of P_i is between 0.4 and 0.7 mM as a result of the hydrolysis and resynthesis of ATP and because of impurities in stock reagents (Pate & Cooke, **1989**). Mg^{2+} was added as $MgCl_2$ with a specified free concentration of 1 mM and Ca^{2+} was added as $CaCl_2$. The ionic strength was adjusted to 180 mM with KCl, and the pH was adjusted to 7.0 or 6.2 with KOH and HCl. The skinning solution was composed of 50% relaxing solution and 50% glycerol (vol:vol).

Experimental set-up

Contractile function experiments were performed on ~2–3 mm long single fibre segments isolated from the muscle biopsy and are referred to as fibres in the present study. On the day of experimentation, a fibre was isolated from the biopsy and the ends secured with 4.0 monofilament posts tied with 10.0 nylon sutures to a force transducer (400A; Aurora Scientific, Aurora, Ontario, CA, USA) and high-speed servomotor (controller 312C; Aurora Scientific) in a plastic chamber containing cold relaxing solution (Moss, **1979**). Once the fibre was attached, the positions of the force transducer and servomotor were adjusted so that the fibre could be suspended in 100–120 µL of relaxing solution cooled to 12°C by a temperature-controlled Peltier unit. The fibre remained in the 12°C relaxing solution, except when transferred either into air for imaging or to a second Peltier unit for activation at 15 or 30°C. To view the fibre at 800× magnification, the microsystem was transferred to the stage of an inverted microscope. The sarcomere length was adjusted to 2.5 µm using a calibrated eyepiece micrometer, and the fibre length measured as the distance between the two points of attachment via a mechanical micrometer (Starrett, Athol, MA, USA). Fibre width was determined from a digital image (CoolSNAP ES; Roper Scientific Photometrics, Tucson, AZ, USA) taken when the fibre was briefly suspended in air (<5 s). The fibre width was measured at three locations along the segment length, and the average fibre diameter and cross-sectional area (CSA) were calculated assuming that the fibre forms a cylinder when in air.

Experimental design

All single fibre contractile experiments began with a sequence of four or five contractions (activating solution – pH 7.0 + 0 mM P_i) to determine the maximal Ca^{2+}-activated P_o and unloaded shortening velocity (V_o) at 15°C. Each fibre was then selected for one of two sets of experiments: (i) V_o and k_{tr} or (ii) force–velocity tests.

For the first set of experiments, k_{tr} was measured at low (15°C) and high (30°C) temperatures under two control conditions (pH 7.0 + 0 mM P_i and pH 7.0 + 4 mM P_i) and an experimental condition mimicking fatigue (pH 6.2 + 30 mM P_i). Fibre V_o was also measured in all three activating conditions at 15°C but with one control condition (pH 7.0 + 4 mM P_i) and the experimental fatigue condition (pH 6.2 + 30 mM P_i) at 30°C. For the fibres selected for the second set of experiments, force–velocity measurements were performed at 15 and 30°C but with only one control condition (pH 7.0 + 4 mM P_i) and the experimental fatigue condition (pH 6.2 + 30 mM P_i). The pH 7.0 + 0 mM P_i control condition was used for comparison with other single fibre experiments in animals (Metzger & Moss, **1990b**; Knuth *et al*. **2006**; Nelson *et al*. **2014**) and humans (D'Antona *et al*. **2003**; Trappe *et al*. **2003**; Frontera *et al*. **2008**; Lamboley *et al*. **2015**), whereas the pH 7.0 + 4 mM P_i control condition was used to more closely mimic the [P_i] in the quiescent human quadriceps muscle (Kemp *et al*. **2007**). Because of the tendency for higher temperatures (>25°C) to damage isolated fibres, all experiments were conducted first at 15°C and then at 30°C. However, within each temperature, the control and experimental fatigue conditions were randomized to alleviate the potential of an order effect. Fibres with visible tears or that had a decrease in the maximal Ca^{2+}-activated isometric tension to <90% of the initial P_o within a condition were excluded from further analysis. Unlike in animal experiments (Debold *et al*. **2004**; Karatzaferi *et al*. **2008**), the fast MHC II fibres from the humans in the present study, particularly from old adults, deteriorated too rapidly to obtain full data sets at 30°C. As a result, data are reported for the fast MHC II fibres at 15°C and the slow MHC I fibres at 15 and 30°C.

V_o and k_{tr} experiments

V_o was determined using the slack test (Edman, **1979**). Fibres were maximally activated in saturating Ca^{2+} (pCa 4.5), allowed to generate P_o, and then rapidly shortened with the servomotor to a predetermined distance so that force was momentarily reduced to zero. The fibre remained activated until the redevelopment of force, after which the fibre was returned to relaxing solution and re-extended to its original position. Fibres were activated four or five times in each condition and slacked at varying distances (100–450 μm at 15°C and 200–450 μm at 30°C), which never exceeded a distance >20% fibre length. The V_o for each condition was the slope of the least squares regression line between the slack distance and the time required to begin the redevelopment of force. The reported P_o was the average from all the contractions within each condition.

To test the effects of age and metabolites (H^+ and P_i) on the low- to high-force transition of the cross-bridge cycle, k_{tr} was measured following a rapid slack re-extension manoeuvre of a maximally Ca^{2+}-activated fibre (Metzger & Moss, **1990a**,*b*). This manoeuvre is similar to the slack test with the addition of the rapid re-extension of the activated fibre, which temporarily dissociates myosin from actin. The slack distance for each fibre was 400–450 μm with the duration prior to re-extension set to 10 ms at 30°C, 20 ms for fibres with a V_o > 2.0 fl s^{-1} at 15°C and 40–60 ms for fibres with a V_o < 2.0 fl s^{-1} at 15°C. Force redevelopment following the re-extension was fit with a first-order exponential function, where k_{tr} is the exponential time constant (s^{-1}) that describes the rate of force redevelopment (Metzger & Moss, **1990b**).

Force–velocity experiments

In the second set of experiments, force–velocity and force–power curves were obtained as described previously (Debold *et al*. **2004**; Nelson *et al*. **2014**). Fibres were maximally activated in saturating Ca^{2+}, allowed to generate P_o and then subjected to three predetermined submaximal isotonic loads (300-FC1 Force Controller; Positron Development, Inglewood, CA, USA). Fibres were activated four to six times in each condition to obtain 12–18 different isotonic loads, and each force–velocity curve was fit with the hyperbolic Hill equation (Hill, **1938**). Absolute (μN fl s^{-1}) and size-specific power (W l^{-1}) were calculated as the product of shortening

velocity (fl s^{-1}) and absolute (μN) and size-specific force (kN m^{-2}), respectively, and the peak fibre power was determined using the fitted parameters from the force–velocity curve (Widrick *et al.* **1996**).

MHC composition

MHC composition of the isolated fibres were determined by SDS-PAGE and silver staining as described previously (Giulian *et al.* **1983**). Briefly, following the contractile experiments, each fibre was solubilized in 80 μL of SDS sample buffer and loaded on a gel made up of a 3% acrylamide/bis (19:1) stacking layer and 5% separating layer. Gels were run for 20–24 h at 4°C (SE600; Hoefer, Holliston, MA, USA), stained, imaged and visually inspected to classify the MHC isoform composition (I, I/IIa, I/IIa/IIx, IIa, IIa/IIx and IIx) of each fibre.

The MHC distribution of the vastus lateralis for each participant was determined by homogenizing a portion of the biopsy sample (>10 mg) in 30× (v/w) RIPA buffer with a protease and phosphatase inhibitor cocktail (Thermo Fisher Scientific, Waltham, MA, USA). The homogenized samples were run in quadruplicate for each participant with SDS-PAGE, and the relative abundance of each MHC isoform (I, IIa and IIx) was quantified using densitometry and averaged over the four runs for each participant. Because of the low abundance of MHC IIx in most participants, we combined the IIa and IIx isoforms for each participant and report the values as MHC II. The amount of thigh lean mass composed of slow MHC I and fast MHC II muscle for each participant (TLM$_{MHC}$) was estimated based on the measured terms in the equation:

$$\mathrm{TLM_{MHC}} = \mathrm{MHC\,(\%)} \times \mathrm{TLM_{Total}}$$

$$\mathrm{TLM_{MHC}} = \mathrm{MHC\,(\%)} \times \mathrm{TLM_{Total}} \quad (3)$$

where MHC (%) is the relative abundance of the MHC isoform (I or II) from the muscle homogenate, and TLM$_{Total}$ is the total thigh lean mass from the DXA scan (Fig. 1). This calculation assumes that the MHC distribution from the biopsy sample of the vastus lateralis is representative of the average distribution of all the quadriceps muscles.
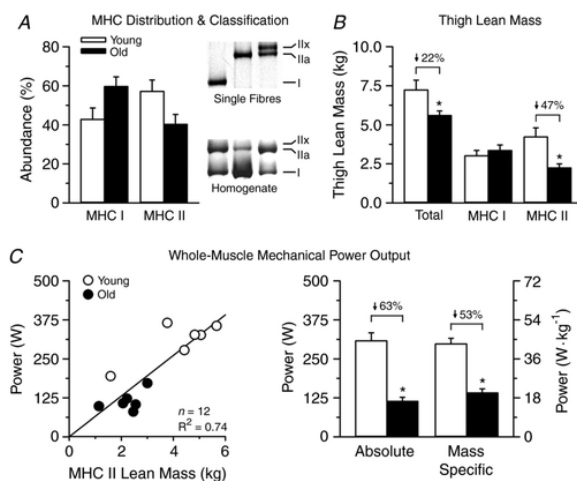

Figure 1. Whole-muscle mechanical power output and MHC distribution in the young and old men

There was a trend ($P = 0.053$) towards a higher relative abundance of MHC I and lower abundance of MHC II in the vastus lateralis muscle of old compared to young adults (*A*). Total thigh lean mass was 22% lower in old compared to young adults, with a selective loss in the fast MHC II lean mass with ageing and no age differences in the slow MHC I lean mass (*B*). Mean absolute mechanical power outputs from the high-velocity exercise were

63% lower in old compared to young adults and remained 53% lower in old adults after correcting for differences in the total thigh lean mass (*C*). Linear regression analyses revealed that the differences in the absolute power outputs with ageing were strongly associated with the differences in the fast MHC II lean mass (*C*). Muscle homogenates in the gel image (5% SDS-PAGE) in (*A*) are from two young adults (outside lanes) and an old adult (middle lane). Gels (5% SDS-PAGE) were also used to classify single fibres based on the MHC isoforms (I, IIa and IIx) following the contractile experiments. Single fibres in the gel image in (*A*) were classified from left-to-right as type I, IIa and hybrid IIa/IIx, respectively. [*]Significantly different compared to young adults (*P* < 0.05). Values are the mean ± SE.

Statistical analysis

Anthropometrics, whole-muscle knee extensor function and MHC distribution were compared between age groups (young and old) using an unpaired *t* test. For the whole-limb experiments, repeated measure ANOVA was performed on the measure of fatigability (reductions in power) and the measurements to identify the sites of fatigue along the motor pathway (voluntary activation, M-wave and electrically-evoked contractile properties). The relative reductions in mechanical power from the beginning to the end of the fatiguing exercise were compared between age groups with an unpaired *t* test. Simple linear regression analyses were performed between the reductions in mechanical power and the measurements to identify the sites of fatigue in the intact neuromuscular system. Statistical analyses for the whole-muscle knee extensor function, fatigability and the MHC distribution were performed using SPSS, version 24.0 (IBM Corp., Armonk, NY, USA).

To test for differences in single fibre morphology and contractile mechanics between the young and old adults, a nested ANOVA was used with age group (young and old) and fibre type (I, IIa, and IIa/IIx) as the fixed factors. No pure MHC IIx, hybrid I/IIa or hybrid I/IIa/IIx fibres were observed in the present study. When a significant main effect of fibre type was observed, pairwise *post hoc* comparisons were performed using Tukey's method. A repeated-measures nested ANOVA was employed to test the effect of temperature (15 and 30°C) and activating condition (pH 7.0 + 0 mM P_i, pH 7.0 + 4 mM P_i, and pH 6.2 + 30 mM P_i) on the contractile mechanics of the different fibre types isolated from young and old adults. Because of the small number of hybrid MHC IIa/IIx fibres tested in the contractile experiments, we grouped the pure MHC IIa with the hybrid MHC IIa/IIx fibres and refer to the grouped data as MHC II. We elected to group the fast MHC fibre types rather than exclude all hybrid MHC IIa/IIx fibres because none of the outcomes differed when the MHC II fibres were grouped *vs.* when the hybrid MHC IIa/IIx were excluded. Statistical analysis for the single fibre morphology and contractile mechanics was performed using Minitab, version 18.0 (Minitab Inc., State College, PA, USA). *P* < 0.05 was considered statistically significant. Data are presented as the mean ± SD in the text and tables and the mean ± SE in the figures.

Results

Whole-muscle knee extensor function, fatigability and MHC distribution

Anthropometrics, PA levels and whole-muscle knee extensor function measurements are shown in Table **1**. The PA levels assessed by triaxial accelerometry did not differ between the young and old adults. As expected, thigh lean mass and absolute isometric torque and mechanical power outputs of the knee extensors were lower in old compared to young adults. After correcting for differences in thigh lean mass, the isometric torque and power outputs remained lower in old adults by 38% and 53%, respectively. Calculations from the MHC distribution analysis (eqn **3**) revealed a lower amount of fast MHC II muscle (Fig. **1**) in old (2.2 ± 0.6 kg) compared to young men (4.2 ± 1.4 kg; *P* = 0.011), which was strongly correlated with the absolute power output

(r = 0.861, P < 0.001) and isometric torque (r = 0.785, P = 0.002) of the knee extensors. By contrast, there was no difference in the slow MHC I thigh lean mass in old (3.4 ± 0.9 kg) compared to young adults (3.0 ± 0.9 kg; P = 0.504), nor was there a correlation between MHC I lean mass and knee extensor power output (r = −0.198, P = 0.537) or isometric torque (r = 0.024, P = 0.940). The fatigability (reductions in power) of the knee extensor muscles was ∼2.7 fold greater in old compared to young adults, with an average relative reduction in power of 32 ± 12% in old compared to 12 ± 13% in young adults.

Table 1. Anthropometrics, knee extensor function and physical activity levels for the young and old men

		Young men (6)	Old men (6)	*P* value
Age	(years)	23.3 ± 3.1	81.5 ± 7.2	**<0.001**
Height	(cm)	178.9 ± 8.9	170.0 ± 7.4	0.089
Weight	(kg)	74.8 ± 11.3	75.8 ± 10.2	0.877
Body mass index	(kg m^{-2})	23.3 ± 1.9	26.2 ± 2.9	0.064
Whole-body fat	(%)	17.6 ± 4.6	30.1 ± 7.7	**0.009**
Whole-body lean mass	(kg)	59.5 ± 9.9	50.5 ± 4.0	0.066
Thigh lean mass	(kg)	7.2 ± 1.5	5.6 ± 1.5	**0.039**
Physical activity	(steps day^{-1})	9,175 ± 4,947	7,977 ± 3,232	0.630
Isometric				
MVC torque	(Nm)	283 ± 59	137 ± 54	**<0.001**
Mass-specific torque	(Nm kg^{-1})	17.9 ± 2.4	11.1 ± 2.2	**<0.001**
Voluntary activation (eqn 1)	(%)	97.9 ± 2.0	96.6 ± 2.3	0.321
Voluntary activation (eqn 2)	(%)	0.4 ± 0.4	0.6 ± 0.4	0.356
Dynamic				
Mechanical power	(W)	308 ± 63	114 ± 31	**<0.001**
Mass-specific power	(W kg^{-1})	42.9 ± 6.5	20.2 ± 4.7	**<0.001**
Angular velocity	(rad s^{-1})	4.5 ± 0.2	3.5 ± 0.3	**<0.001**
Fatigability - power	(% Δ)	−12 ± 13	−32 ± 12	**0.019**
Femoral nerve stimulation				
Twitch torque (Q_{tw})	(Nm)	59.4 ± 11.5	38.2 ± 6.2	**0.003**
Rate of torque development (dT/dt)	(Nm s^{-1})	1,267 ± 324	722 ± 129	**0.007**
1/2 Relaxation time	(ms)	71 ± 16	76 ± 23	0.675
VL M_{max}	(mV)	18.0 ± 1.7	7.5 ± 2.7	**<0.001**
VL M-wave area	(mV ms)	101.0 ± 9.5	51.5 ± 17.9	**<0.001**

Body fat percentage and lean mass were measured via dual X-ray absorptiometry, and physical activity was measured via triaxial accelerometry. MVC torque was the highest torque output recorded from the MVC attempts in the experimental session. Voluntary activation was assessed by TMS to the motor cortex and was the median from the five sets of MVC-60–80% contractions performed prior to the dynamic exercise. Mechanical power was the highest average obtained from five sequential contractions of the first 10 contractions performed during the dynamic fatiguing exercise. Mass-specific torque and power were calculated with the thigh lean mass. Variables from electrical stimulation to the femoral nerve were the median values from the stimuli delivered at rest following the MVC and 80% MVC contractions. M_{max} for the vastus lateralis (VL) was the peak-to-peak maximal compound muscle action potential amplitude. The sample size (n) for each cohort is reported in parentheses. A significant age difference at P < 0.05 is indicated in bold. Values are the mean ± SD.

Voluntary activation

Baseline voluntary activation calculated using the estimated resting twitch (eqn 1) and only the superimposed twitch (eqn 2) did not differ between young and old adults (Table 1). Furthermore, the ability to volitionally activate the knee extensor muscles immediately following the fatiguing exercise did not change compared to baseline for young (eqn 1: P = 0.709; eqn 2: P = 0.644) or old adults (eqn 1: P = 0.293; eqn 2: P = 0.548).

Neuromuscular propagation (M-wave)

Baseline M-wave peak-to-peak amplitudes (M_{max}) and areas for the vastus lateralis are presented in Table [1]. Despite larger baseline vastus lateralis M_{max} and M-wave areas in young compared to old men, both variables did not change following the fatiguing exercise for either age group ($P > 0.05$).

Electrically-evoked contractile properties

Baseline contractile properties elicited by electrical stimulation to the femoral nerve are also presented in Table [1]. The amplitude of the Q_{tw} decreased following the fatiguing exercise by $23 \pm 15\%$ in young ($P = 0.008$) and $30 \pm 9\%$ in old adults ($P < 0.001$). Similarly, the dT/dt decreased by $21 \pm 18\%$ in young ($P = 0.023$) and $37 \pm 13\%$ in old adults ($P = 0.002$), whereas the half-relaxation time increased following the fatiguing exercise by $22 \pm 18\%$ in young ($P = 0.036$) and $94 \pm 59\%$ in old adults ($P = 0.004$). Regression analyses revealed that the relative changes in all contractile properties were strongly associated with the relative reductions in power output during the fatiguing exercise: Q_{tw} ($r = 0.82$; $P = 0.001$), dT/dt ($r = 0.89$; $P < 0.001$) and half-relaxation time ($r = -0.68$; $P = 0.014$). However, the most closely associated variable was the reduction in the rate of torque development (dT/dt), which explained 79% of the variance in the loss in power during the fatiguing exercise (Fig. [2]).
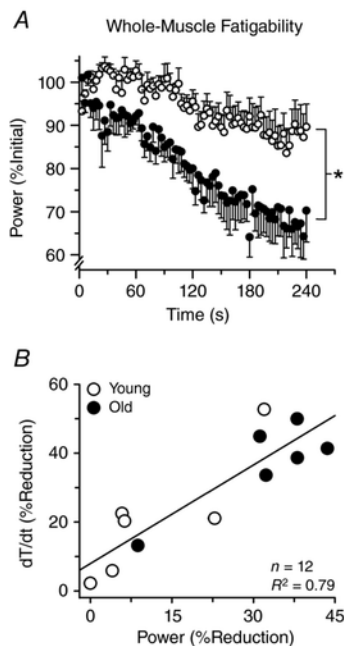

Figure 2. Fatigability (reductions in power) of the knee extensors during a high-velocity fatiguing exercise in young and old men

The fatigability of the knee extensor muscles was ~2.7 fold greater in the old compared to young adults, with an average relative reduction in power of 32% in the old compared to 12% in the young (A). Regression analyses revealed that the relative reductions in mechanical power were best predicted by the relative reductions in the rates of torque development (dT/dt) from the electrically-evoked twitches (B). *Significantly different compared to young adults ($P < 0.05$). Values are the mean ± SE.

Single fibre morphology and contractile mechanics

Table [2] shows the fibre diameter, cross-sectional area (CSA), P_o and V_o at 15°C (pH 7.0 + 0 mM P_i) for all 254 fibres studied (young = 122 and old = 132). The CSA of MHC I fibres did not differ between young and old adults

($P = 0.415$). Similarly, absolute P_o ($P = 0.455$) and size-specific P_o ($P = 0.717$) did not differ for MHC I fibres with age. However, the CSA of both MHC IIa and IIa/IIx fibres was 59% and 54% smaller in fibres from old compared to young adults ($P < 0.001$). Accordingly, the absolute P_o was 52% and 50% lower for MHC IIa and IIa/IIX fibres from old compared to young adults ($P < 0.001$). The differences in absolute P_o were explained entirely by the differences in fibre CSA as indicated by the greater size-specific P_o in old compared to young adults for the MHC IIa ($P = 0.002$) and no age differences for the MHC IIa/IIx fibres ($P = 0.146$). Independent of age, the size-specific P_o of MHC I fibres (183 ± 27 kN m^{-2}) was 17% lower than MHC IIa fibres (220 ± 39 kN m^{-2}) and 24% lower than MHC IIa/IIx fibres (243 ± 41 kN m^{-2}) ($P < 0.001$), with no differences between IIa and IIa/IIx fibres ($P = 0.676$).

Table 2. P_o and V_o in pH 7.0 + 0 mM P$_i$ activating solution at 15°C

		Young	Old	Difference
Slow MHC I	*n*	56	59	
Diameter	μm	85.4 ± 14.4	77.7 ± 17.2	↔
Cross-Sectional Area	μm^2	5,890 ± 1,890	4,965 ± 2,139	↔
Absolute P$_o$	mN	1.05 ± 0.32	0.90 ± 0.37	↔
Size-Specific P$_o$	kN m^{-2}	180.5 ± 25.7	185.9 ± 28.3	↔
Shortening Velocity (V_o)	fl s^{-1}	1.38 ± 0.41	1.24 ± 0.24	↔
Fast MHC IIa	*n*	60	53	
Diameter	μm	99.7 ± 10.9	62.8 ± 13.8	↓ 37%
Cross-Sectional Area	μm^2	7,895 ± 1,597	3,249 ± 1,464	↓ 59%
Absolute P$_o$	mN	1.57 ± 0.27	0.76 ± 0.30	↓ 52%
Size-Specific P$_o$	kN m^{-2}	202.4 ± 26.2	240.9 ± 40.4	↑ 19%
Shortening Velocity (V_o)	fl s^{-1}	4.03 ± 1.05	3.89 ± 0.91	↔
Fast MHC IIa/IIx	*n*	6	20	
Diameter	μm	81.0 ± 8.6	54.7 ± 8.2	↓ 32%
Cross-Sectional Area	μm^2	5,200 ± 1,150	2,402 ± 700	↓ 54%
Absolute P$_o$	mN	1.17 ± 0.20	0.58 ± 0.16	↓ 50%
Size-Specific P$_o$	kN m^{-2}	227.4 ± 24.0	247.3 ± 44.6	↔
Shortening Velocity (V_o)	fl s^{-1}	5.31 ± 0.84	6.01 ± 1.89	↔

Fibre diameter and CSA were calculated from a digital image taken when the fibre was briefly suspended in air (<5 s). P_o and V_o were measured from the slack test. The number of fibres (*n*) is reported for each fibre type from both young and old adults. The percentage difference between young and old for each MHC isoform is reported when $P < 0.05$. Values are the mean ± SD.

V_o did not differ between fibres from young and old adults for MHC I ($P = 0.215$), IIa ($P = 0.537$) or IIa/IIx fibres ($P = 0.440$). Independent of age, V_o was 67% slower in MHC I (1.31 ± 0.34 fl s^{-1}) compared to IIa fibres (3.96 ± 0.98 fl s^{-1}; $P < 0.001$) and 32% slower in MHC IIa compared to IIa/IIx fibres (5.85 ± 1.72 fl s^{-1}; $P < 0.001$).

Effects of P$_i$ and H$^+$ on single fibre contractile mechanics

P$_o$

The absolute P_o of fibres from young and old adults for all testing conditions is shown in Fig. **3**. For fast MHC II fibres from young adults, P_o at 15°C was reduced by $23 \pm 3\%$ and $54 \pm 3\%$ in the 4 mM P$_i$ (1.19 ± 0.23 mN) and fatigue (0.71 ± 0.14 mN) conditions compared to 0 mM P$_i$ (1.54 ± 0.28 mN) ($P < 0.001$). Similarly, the P_o of MHC II fibres from old adults was reduced by $25 \pm 5\%$ and $57 \pm 4\%$ in the 4 mM P$_i$ (0.54 ± 0.22 mN) and fatigue (0.31 ± 0.14 mN) conditions compared to 0 mM P$_i$ (0.72 ± 0.29 mN) ($P < 0.001$). Although the P$_i$- and H$^+$-induced

reductions in P_o did not differ with age, the absolute P_o of old adult MHC II fibres in all conditions was 53–56% lower than the P_o of young MHC II fibres ($P < 0.001$). The lower P_o in MHC II fibres with age was because of the smaller CSA in fibres from old compared to young adults.
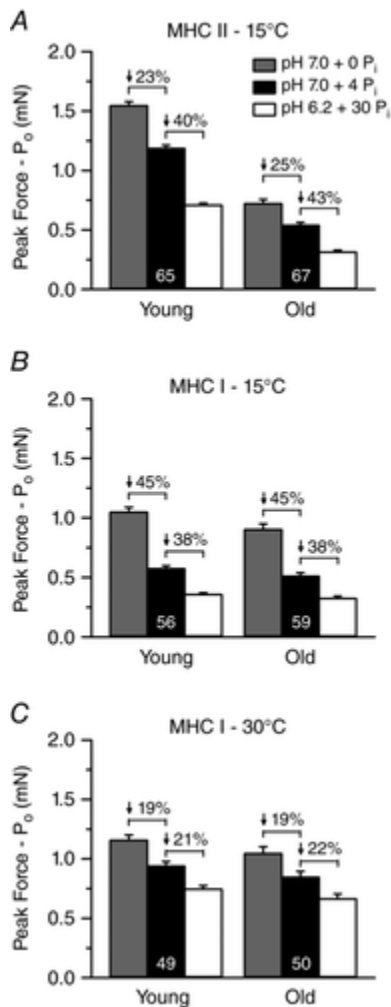

Figure 3. P_o of single fibres from young and old men

P_o was lower in the 4 mM P_i control condition compared to the 0 mM P_i control condition, and was lower in the fatigue condition (pH 6.2 + 30 mM P_i) compared to both control conditions for the MHC II at 15°C (*A*) and MHC I at 15°C (*B*) and 30°C (*C*). However, the relative decrease in peak isometric force elicited by P_i and H^+ was similar in fibres isolated from young and old adults for both fibre types and all conditions. Values are the mean ± SE, with the number of fibres (*n*) displayed within the bars.

Independent of age, the relative reductions in P_o elicited by the 4 mM P_i and fatigue conditions in slow MHC I fibres at 15°C were greater than the reductions observed in MHC II fibres (Fig. **3**). For the young adult MHC I fibres, P_o was reduced by 45 ± 4% and 66 ± 4% in the 4 mM P_i (0.57 ± 0.19 mN) and fatigue (0.36 ± 0.11 mN) conditions compared to 0 mM P_i (1.05 ± 0.32 mN) ($P < 0.001$). Similar to the findings from fast MHC II fibres, there was no age difference for the P_i- and H^+-induced decrements in P_o for slow MHC I fibres from young and old adults. Specifically, compared to 0 mM P_i (0.90 ± 0.36 mN), the P_o of MHC I fibres from old adults was reduced by 45 ± 6% and 66 ± 4% in the 4 mM P_i (0.51 ± 0.24 mN) and fatigue (0.32 ± 0.16 mN) conditions, respectively ($P < 0.001$).

Increasing the temperature from 15 to 30°C resulted in an increase in MHC I fibre P_o of 15 ± 8%, 72 ± 20%, and 119 ± 35% in the 0 mM P_i, 4 mM P_i and fatigue conditions, respectively. The greater increases in P_o in the 4 mM P_i and fatigue conditions resulted in a reduced P_i- and H^+-induced effect on P_o at 30 compared to 15°C. However, the findings at 30°C remained qualitatively similar to the findings from 15°C, with no age differences observed in the P_i- and H^+-induced decrements in P_o at 30°C (Fig. **3**). Independent of age, P_o was reduced by 19 ± 4% and 37 ± 3% in the 4 mM P_i (0.89 ± 0.32 mN) and fatigue (0.70 ± 0.26 mN) conditions compared to 0 mM P_i (1.10 ± 0.37 mN) ($P < 0.001$)

ktr

The k_{tr} of the fibres from young and old adults for all conditions is shown in Fig. **4**. For MHC II fibres at 15°C, there was no age difference in k_{tr} in the 0 mM P_i (young = 9.5 ± 1.4 s^{-1}, old = 10.4 ± 2.7 s^{-1}; $P = 0.597$), 4 mM P_i (young = 11.4 ± 1.7 s^{-1}, old = 11.6 ± 3.0 s^{-1}; $P = 0.950$) or fatigue (young = 7.8 ± 1.2 s^{-1}, old = 8.0 ± 2.0 s^{-1}; $P = 0.838$) conditions. Independent of age, k_{tr} was 15 ± 8% higher in the 4 mM P_i compared to the 0 mM P_i ($P < 0.001$) condition and was reduced by 20 ± 9% and 31 ± 7% in the fatigue compared to the 0 and 4 mM P_i conditions, respectively ($P < 0.001$).
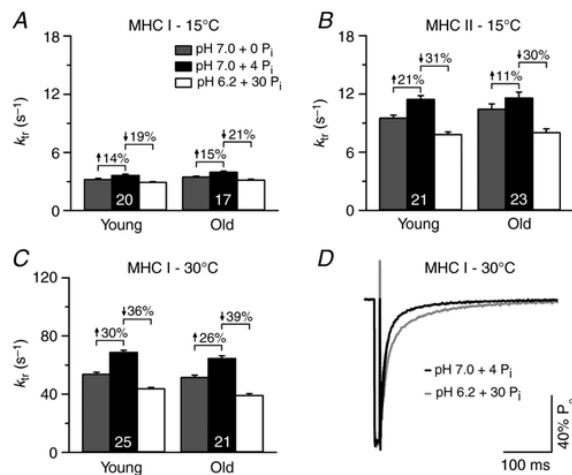

Figure 4. k_{tr} of single fibres from young and old men

k_{tr} was accelerated in the 4 mM P_i control condition compared to the 0 mM P_i control condition for the MHC I at 15°C (*A*) and 30°C (*C*) and MHC II at 15°C (*B*). By contrast, the fatigue condition (pH 6.2 + 30 mM P_i) decreased k_{tr} compared to both control conditions for both fibre types, and did so similarly in fibres isolated from young and old adults. The k_{tr} of MHC I fibres increased 18-fold with an increase in temperature from 15 to 30°C in the 4 mM P_i control condition (*C*), and the effect of the fatigue condition was exacerbated by the increase in temperature. Shown in (*D*) are representative force redevelopment (k_{tr}) traces that were normalized to the peak isometric force (%P_o) for a MHC I fibre isolated from an 84-year-old in both control (pH 7.0 + 4 mM P_i) and fatigue (pH 6.2 + 30 mM P_i) conditions at 30°C. Traces are superimposed to compare the differences between the two conditions. Values are the mean ± SE, with the number of fibres (*n*) displayed within the bars.

The k_{tr} of MHC I fibres was ∼3-fold slower than the k_{tr} of MHC II fibres for all three conditions at 15°C. Similar to the findings from MHC II fibres at 15°C, there was no age difference in k_{tr} of MHC I fibres in the 0 mM P_i (young = 3.2 ± 0.5 s^{-1}, old = 3.5 ± 0.4 s^{-1}; $P = 0.279$), 4 mM P_i (young = 3.6 ± 0.6 s^{-1}, old = 4.0 ± 0.5 s^{-1}; $P = 0.161$) or fatigue (young = 2.9 ± 0.4 s^{-1}, old = 3.1 ± 0.4 s^{-1}; $P = 0.108$) conditions. Also similar to the findings from MHC II fibres, the k_{tr} for MHC I fibres increased by 14 ± 10% in the 4 mM P_i compared to the 0 mM P_i ($P < 0.001$) condition and was reduced by 8 ± 11% and 20 ± 6% in the fatigue compared to the 0 and

4 mM P_i conditions, respectively ($P < 0.001$). The reductions in k_{tr} elicited by the fatigue condition were greater in MHC II compared to MHC I fibres ($P < 0.001$).

The k_{tr} of MHC I fibres increased 14- to 18-fold with the increase in temperature from 15 to 30°C for all three conditions. There was no age difference in k_{tr} of MHC I fibres at 30°C in the 0 mM P_i (young = 53.6 ± 7.5 s^{-1}, old = 51.4 ± 7.8 s^{-1}; $P = 0.782$) or 4 mM P_i (young = 68.7 ± 7.7 s^{-1}, old = 64.4 ± 8.6 s^{-1}; $P = 0.261$) conditions, but the absolute k_{tr} in the fatigue condition was lower in fibres from old (39.1 ± 5.8 s^{-1}) compared to young adults (43.6 ± 5.3 s^{-1} $P = 0.049$). The relative reduction in k_{tr} elicited by the fatigue condition, however, did not differ with age ($P = 0.140$). Independent of age, k_{tr} was 28 ± 14% higher in the 4 mM P_i compared to 0 mM P_i ($P < 0.001$) condition and was reduced by 20 ± 13% and 38 ± 6% in the fatigue compared to the 0 and 4 mM P_i conditions, respectively ($P < 0.001$). Unlike the reduced effects of P_i and H$^+$ on P_o at 30 compared to 15°C, the P_i- and H$^+$-induced effects on the absolute and relative changes in k_{tr} were exacerbated with the increase in temperature (Fig. **4**).

Vo

V_o of the fibres from young and old adults for all conditions is shown in Fig. **5**. For MHC II fibres at 15°C, there was no age difference in V_o in the 0 mM P_i (young = 3.79 ± 1.07 fl s^{-1}, old = 3.83 ± 1.09 fl s^{-1}; $P = 0.972$), 4 mM P_i (young = 3.78 ± 1.09 fl s^{-1}, old = 3.84 ± 1.08 fl s^{-1}; $P = 0.908$) or fatigue (young = 2.04 ± 0.41 fl s^{-1}, old = 2.06 ± 0.46 fl s^{-1}; $P = 0.937$) conditions. Independent of age, the fatigue condition elicited a 45 ± 9% reduction in V_o compared to both the 0 and 4 mM P_i conditions ($P < 0.001$). For MHC I fibres at 15°C, there was also no age difference in V_o in the 0 mM P_i (young = 1.18 ± 0.36 fl s^{-1}, old = 1.10 ± 0.23 fl s^{-1}; $P = 0.972$), 4 mM P_i (young = 1.19 ± 0.34 fl s^{-1}, old = 1.11 ± 0.23 fl s^{-1}; $P = 0.908$) or fatigue (young = 0.82 ± 0.18 fl s^{-1}, old = 0.81 ± 0.15 fl s^{-1}; $P = 0.937$) conditions. Also similar to the findings from MHC II fibres, the V_o of MHC I fibres was reduced by 26 ± 12% and 28 ± 11% in the fatigue compared to the 0 and 4 mM P_i conditions, respectively ($P < 0.001$). However, the absolute and relative reductions in V_o in fast MHC II fibres were greater than that occurring in slow MHC I fibres ($P < 0.001$).
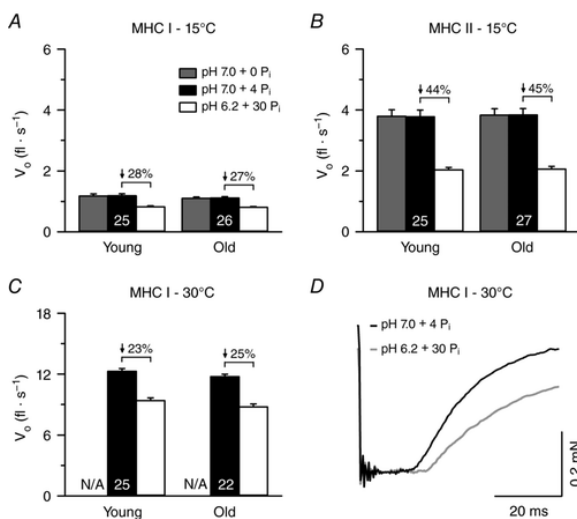

Figure 5. V_o of single fibres from young and old men

V_o did not differ between the two control conditions (pH 7.0 + 0 mM P_i and pH 7.0 + 4 mM P_i) for the MHC I (*A*) or MHC II fibres at 15°C (*B*). By contrast, the fatigue condition (pH 6.2 + 30 mM P_i) decreased V_o compared to both control conditions for both fibre types, and did so similarly in fibres isolated from young and old adults. The V_o of MHC I fibres increased 11-fold with an increase in temperature from 15 to 30°C in the control condition (*C*), but

the effect of the fatigue condition was unaltered by temperature. Shown in (*D*) are representative slack traces with a slack distance of 450 μm for a MHC I fibre isolated from an 84-year-old in both the control (pH 7.0 + 4 mM P_i) and fatigue (pH 6.2 + 30 mM P_i) conditions at 30°C. Traces are superimposed to compare the differences between the two conditions. Values are the mean ± SE, with the number of fibres (*n*) displayed within the bars.

The V_o of the MHC I fibres increased ~11-fold with the increase in temperature from 15 to 30°C for both the 4 mM P_i and fatigue conditions. The V_o of MHC I fibres at 30°C was significantly lower in fibres from old (11.74 ± 1.13 fl s^{-1}) compared to young adults in the 4 mM P_i condition (12.27 ± 1.32 fl s^{-1}; *P* = 0.021) but did not differ with age in the fatigue condition (young = 9.38 ± 1.35 fl s^{-1}, old = 8.78 ± 1.28 fl s^{-1}; *P* = 0.144). In addition, the relative reductions in V_o elicited by the fatigue condition did not differ with age (*P* = 0.567). Unlike the reduced effect observed in the fatigue condition on P_o at 30 compared to 15°C, the relative reductions in V_o were unaffected by the increase in temperature.

Force–velocity curves and peak power

Force–velocity and force–power curves for MHC II fibres from young and old adults at 15°C are shown in Fig. **6**, with key parameters reported in Table **3**. In the 4 mM P_i condition, the maximal shortening velocity calculated from the Hill equation (V_{max}; *P* = 0.684) and the curvature of the force–velocity relationship (a/P_o; *P* = 0.233) did not differ in MHC II fibres with age. By contrast, the absolute P_o (young = 1.23 ± 0.20 mN, old = 0.56 ± 0.19 mN; *P* < 0.001) and peak power (*P* = 0.001) were 50–55% lower in fibres from old compared to young adults. The age differences in absolute P_o and peak power, however, were explained entirely by the differences in fibre CSA as indicated by the 18% and 35% greater size-specific P_o (young = 158 ± 20 kN m^{-2}, old = 186 ± 36 kN m^{-2}; *P* = 0.012) and peak power (*P* = 0.043) (Table **3**) observed in old compared to young adults. The fatigue condition decreased all parameters of the force–velocity relationship compared to the 4 mM P_i condition for MHC II fibres from young and old men (*P* < 0.001), including P_o (−41 ± 5%), V_{max} (−16 ± 9%), peak power (−57 ± 5%) and a/P_o (−14 ± 16%), with no age differences in the relative reductions for any of the measurements (Table **3**).
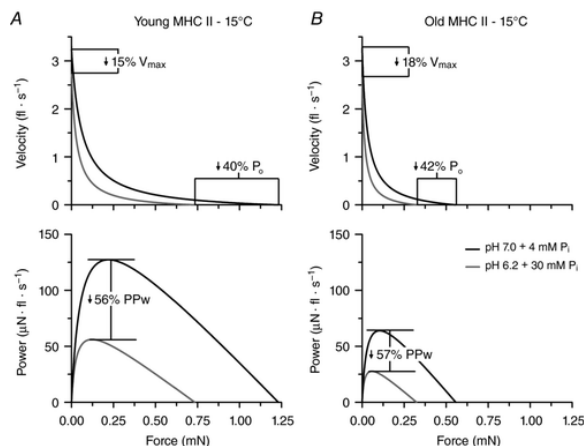

Figure 6. Force–velocity and force–power curves of fast MHC II fibres from young and old men at 15°C

Absolute peak fibre power (PPw) and P_o of the fast MHC II fibres from young adults (*A*) were ~2-fold greater than in fibres from old adults (*B*). The fatigue condition (pH 6.2 + 30 mM P_i) caused significant decreases in V_{max}, P_o and peak power (PPw) compared to the control condition (pH 7.0 + 4 mM P_i) in fibres from young and old adults; however, the relative reductions did not differ with age. The variances around the mean curves were omitted for clarity and are shown in Table **3**.

Table 3. Force–velocity parameters and peak power (PPw) of fast MHC II fibres

		Young (40)	Old (40)	Difference
Absolute PPw (µN fl s^{-1})				
pH 7.0 + 4 mM P_i	15°C	127.3 ± 27.6	63.9 ± 21.2	↓ 50%
pH 6.2 + 30 mM P_i	15°C	56.1 ± 14.1	27.7 ± 10.2	↓ 51%
% Change		−56 ± 4	−57 ± 4	↔
Size−Specific PPw (W l^{-1})				
pH 7.0 + 4 mM P_i	15°C	16.5 ± 3.8	22.2 ± 7.9	↑ 35%
pH 6.2 + 30 mM P_i	15°C	7.3 ± 1.9	9.5 ± 3.6	↔
% Change		−56 ± 5	−57 ± 5	↔
V_{max} (fl s^{-1})				
pH 7.0 + 4 mM P_i	15°C	3.24 ± 0.81	3.27 ± 0.78	↔
pH 6.2 + 30 mM P_i	15°C	2.76 ± 0.69	2.66 ± 0.55	↔
% Change		−15 ± 8	−18 ± 10	↔
a/P_o				
pH 7.0 + 4 mM P_i	15°C	0.05 ± 0.01	0.06 ± 0.02	↔
pH 6.2 + 30 mM P_i	15°C	0.04 ± 0.01	0.05 ± 0.02	↔
% Change		−17 ± 12	−12 ± 18	↔

Absolute (µN fl s⁻¹) and size-specific (W l⁻¹) peak fibre power (PPw) were calculated with the fitted-parameters from the force-velocity curves. V_{max} was calculated using the hyperbolic Hill equation, and the a/P_o ratio is a unitless parameter describing the curvature of the force-velocity relationship. The number of fibres (*n*) for each cohort is reported in parentheses. The relative difference between the control (pH 7.0 + 4 mM P_i) and fatigue (pH 6.2 + 30 mM P_i) condition is reported when $P < 0.05$. The percentage difference between young and old is reported when $P < 0.05$. Values are the mean ± SD.

Figures **7** and **8** show the mean force–velocity and force–power curves for MHC I fibres from young and old adults at 15 and 30°C, respectively, with key parameters reported in Table **4**. In the 4 mM P_i condition at 15°C, there were no age differences in any of the force–velocity parameters (Fig. **7** and Table **4**). The fatigue condition significantly decreased P_o (−37 ± 6%), V_{max} (−14 ± 8%) and peak power (-48 ± 6%) ($P < 0.001$) but did not alter a/P_o ($P = 0.283$), and no age differences were observed in the relative reductions for any of the measurements (Fig. **7**). Independent of age, the relative reductions in P_o and peak power elicited by the fatigue condition were greater in MHC II compared to MHC I fibres ($P < 0.001$), but the reductions in V_{max} did not differ between fibre types ($P = 0.356$).
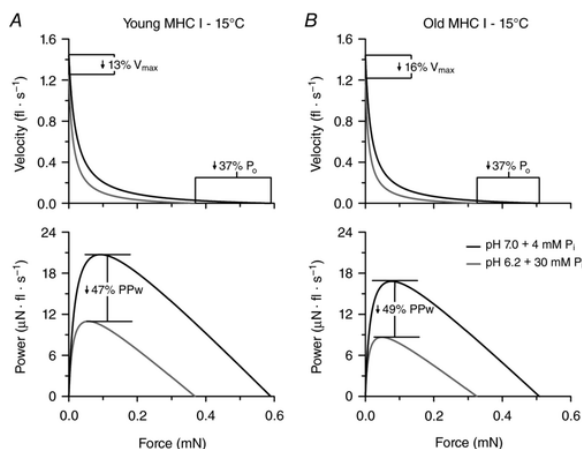
Figure 7. Force–velocity and force–power curves of slow MHC I fibres from young and old men at 15°C

The fatigue condition (pH 6.2 + 30 mM P_i) caused significant decreases in V_{max}, P_o and peak power (PPw) compared to the control condition (pH 7.0 + 4 mM P_i) in MHC I fibres from young (*A*) and old adults (*B*); however, the relative reductions did not differ with age. The variances around the mean curves were omitted for clarity and are shown in Table 4.

Figure 8. Force–velocity and force–power curves of slow MHC I fibres from young and old men at 30°C

The fatigue condition (pH 6.2 + 30 mM P_i) caused significant decreases in V_{max}, P_o and peak power (PPw) compared to the control condition (pH 7.0 + 4 mM P_i) in MHC I fibres from young (*A*) and old adults (*B*); however, the relative reductions did not differ with age. The variances around the mean curves were omitted for clarity and are shown in Table 4.
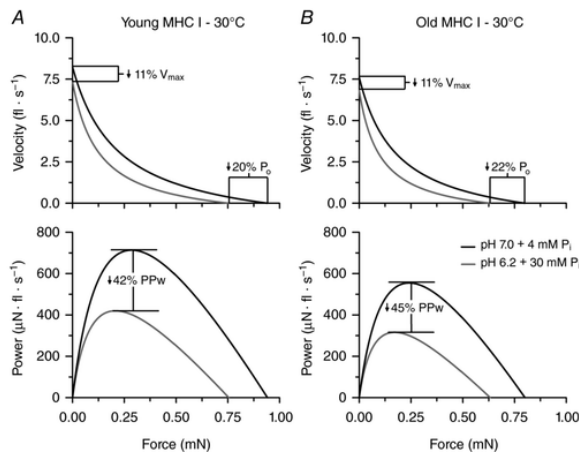
Table 4. Force–velocity parameters and peak power (PPw) of slow MHC I fibres

		Young (30)	Old (32)	Difference
Absolute PPw (μN fl s^{-1})				
pH 7.0 + 4 mM P_i	15°C	20.7 ± 8.3	16.8 ± 6.6	↔
pH 6.2 + 30 mM P_i	15°C	11.0 ± 4.2	8.6 ± 3.6	↔
% Change		− 47 ± 5	− 49 ± 7	↔
pH 7.0 + 4 mM P_i	30°C	713.3 ± 278.0	555.6 ± 268.2	↔
pH 6.2 + 30 mM P_i	30°C	419.9 ± 177.7	315.8 ± 174.0	↔
% Change		− 42 ± 7	− 45 ± 7	↔
Size-Specific PPw (W l^{-1})				
pH 7.0 + 4 mM P_i	15°C	3.7 ± 0.6	3.7 ± 0.8	↔
pH 6.2 + 30 mM P_i	15°C	2.0 ± 0.3	1.9 ± 0.3	↔
% Change		− 47 ± 5	− 49 ± 7	↔
pH 7.0 + 4 mM P_i	30°C	127.8 ± 21.1	120.3 ± 27.0	↔
pH 6.2 + 30 mM P_i	30°C	73.9 ± 14.2	66.9 ± 19.3	↔
% Change		− 42 ± 7	− 45 ± 7	↔
V_{max} (fl s^{-1})				
pH 7.0 + 4 mM P_i	15°C	1.44 ± 0.16	1.44 ± 0.22	↔
pH 6.2 + 30 mM P_i	15°C	1.25 ± 0.16	1.21 ± 0.16	↔
% Change		− 13 ± 7	− 16 ± 8	↔
pH 7.0 + 4 mM P_i	30°C	8.23 ± 0.64	7.61 ± 1.00	↔
pH 6.2 + 30 mM P_i	30°C	7.34 ± 0.85	6.82 ± 1.32	↔
% Change		− 11 ± 8	− 11 ± 11	↔
a/P_o				
pH 7.0 + 4 mM P_i	15°C	0.03 ± 0.00	0.03 ± 0.01	↔
pH 6.2 + 30 mM P_i	15°C	0.03 ± 0.01	0.03 ± 0.01	↔

% Change		$\leftrightarrow$	$\leftrightarrow$	$\leftrightarrow$
pH 7.0 + 4 mM P_i	30°C	0.23 ± 0.03	0.22 ± 0.05	$\leftrightarrow$
pH 6.2 + 30 mM P_i	30°C	0.16 ± 0.03	0.15 ± 0.03	$\leftrightarrow$
% Change		− 27 ± 14	− 31 ± 9	$\leftrightarrow$

Absolute (μN fl s^{-1}) and size-specific (W l^{-1}) peak fibre power (PPw) were calculated with the fitted-parameters from the force-velocity curves. V_{max} was calculated using the hyperbolic Hill equation, and the a/P_o ratio is a unitless parameter describing the curvature of the force-velocity relationship. A lower a/P_o ratio indicates greater curvature of the force-velocity relationship. The number of fibres (n) for each cohort is reported in parentheses. The relative difference between the control (pH 7.0 + 4 mM P_i) and fatigue (pH 6.2 + 30 mM P_i) conditions is reported when $P < 0.05$. Values are the mean ± SD.

Increasing temperature from 15 to 30°C increased all parameters of the force–velocity relationship in the 4 mM P_i condition ($P < 0.001$), including P_o (62 ± 14%), V_{max} (455 ± 80%), peak power (3,285 ± 568%) and a/P_o (563 ± 135%). Similar to the results from MHC I fibres at 15°C, there were no age differences for any force–velocity parameters in 4 mM P_i at 30°C (Fig. **8** and Table **4**). However, the fatigue condition significantly decreased all parameters of the force–velocity relationship compared to the 4 mM P_i condition ($P < 0.001$), including P_o (–21 ± 3%), V_{max} (–11 ± 10%), peak power (–43 ± 7%) and a/P_o (–29 ± 12%), with no age differences in the relative reductions for any of the measurements (Table **4**). Independent of age, the relative reductions in P_o ($P < 0.001$), peak power ($P = 0.001$) and V_{max} ($P = 0.041$) elicited by the fatigue condition were less at 30 compared to 15°C.

Discussion

The present study aimed to determine the mechanisms for the loss in muscle power and increased fatigability with ageing by integrating measures of whole-muscle knee extensor function with single fibre contractile mechanics. We observed marked atrophy of fast MHC II fibres in old compared to young men that corresponded closely with our estimates of the total thigh lean mass composed of MHC II compared to MHC I muscle (eqn **3**). The lower MHC II lean mass was strongly associated with the age differences in isometric torque and power output, suggesting that the age-related loss in knee extensor function is due, in large part, to the selective atrophy and/or loss of fast MHC II fibres. Despite a lower amount of the more fatigable MHC II muscle with age, the relative reduction in power during the high-velocity knee extension exercise was ~2.7-fold greater in old compared to young men. We confirmed previous findings from non-human studies (Cooke *et al*. **1988**; Karatzaferi *et al*. **2008**; Nelson *et al*. **2014**) that elevated levels of H$^+$ (pH 6.2) and P_i (30 mM) act synergistically to depress cross-bridge function by inhibiting isometric force (P_o), shortening velocity (V_o and V_{max}), peak power and the low-to high-force transition of the cross-bridge cycle. However, the depressive effects of these ions in saturating Ca^{2+} conditions were similar in fibres from old compared to young men, suggesting that the age-related increase in fatigability during dynamic exercise cannot be attributed to an increased sensitivity of the cross-bridge to H$^+$ and P_i.

Age-related increases in fatigability and decreases in strength and power are determined primarily by changes within the muscle

The older men in the present study demonstrated hallmark signs of ageing of the knee extensor muscles, which included a 22% lower thigh lean mass, 54% lower maximal isometric strength, 63% lower mechanical power output (Fig. **1**) and an ~2.7-fold increase in fatigability during a high-velocity exercise compared to the younger

men (Fig. 2). The accelerated age-related loss in strength and power relative to the loss in muscle mass is often observed in ageing studies and is commonly referred to as a decrease in 'muscle quality' (Doherty, 2003; Reid & Fielding, 2012; Russ *et al*. 2012). Despite its widespread recognition, the primary mechanisms responsible for the age-related loss in 'muscle quality' remain elusive. Our data, which integrated measures of whole-muscle knee extensor function with single cell contractile properties, shed light on this unanswered question and revealed that the loss in muscle strength and power with age was determined primarily by the selective atrophy of fast MHC II fibres.

Multiple mechanisms have been proposed to explain the decrease in 'muscle quality' with ageing, including decreased voluntary neural drive (Russ *et al*. 2012; Venturelli *et al*. 2015), infiltration of adipose and connective tissue into the muscle (Lexell, 1995; Kent-Braun *et al*. 2000), motor unit remodelling and instability of the neuromuscular junction (Hepple & Rice, 2016; Hunter *et al*. 2016), and/or impaired cross-bridge mechanics and Ca^{2+} handling (Frontera *et al*. 2000; Miller & Toth, 2013; Lamboley *et al*. 2015; Lamboley *et al*. 2016; Power *et al*. 2016). In the present study, the ability of the older men to activate the knee extensors during a maximal voluntary isometric contraction was not different compared to the young men. These findings are in agreement with a majority of other studies on both dynamic and isometric contractions that report no age differences in voluntary activation when older participants are provided practice and familiarization to the procedures (Klass *et al*. 2007; Hunter *et al*. 2016; Rozand *et al*. 2017). Similarly, we found no age differences in any contractile properties of the isolated fibres, other than a lower absolute P_o and power output in MHC II fibres from old compared to young adults (Figs 3 and 6). However, when the differences in absolute P_o and peak power were normalized to the differences in fibre size, old adult MHC II fibres generated higher size-specific force and power compared to the young adult fibres (Tables 2 and 3). The preservation or even increase in size-specific fibre force and power with ageing is in agreement with a large number of studies (Trappe *et al*. 2003; Korhonen *et al*. 2006; Frontera *et al*. 2008; Slivka *et al*. 2008; Miller *et al*. 2013; Venturelli *et al*. 2015; Grosicki *et al*. 2016) but in contrast to others (Larsson *et al*. 1997; Frontera *et al*. 2000; Lamboley *et al*. 2015; Power *et al*. 2016). The explanation for the disparities between studies is unknown, but clearly, when corrected for changes from the atrophy of fast MHC II fibres, single fibre contractile function was not impaired in our old participants who had physical activity levels similar to the young participants.

An alternative hypothesis that may explain the age-related loss in strength and power is attributed not to a decrease in 'muscle quality' *per se* but, instead, to the selective atrophy of muscle expressing the MHC II isoform. Because MHC II fibres generate higher size-specific force and power compared to MHC I fibres (Tables 2-4) (Trappe *et al*. 2003; Miller *et al*. 2015; Grosicki *et al*. 2016), a selective loss and atrophy of MHC II fibres would be consistent with a more rapid loss in both isometric strength and power production with age. Accordingly, we observed a trend ($P = 0.053$) towards a 17% lower relative abundance of MHC II in the vastus lateralis of old compared to young men. However, what is more important for the absolute isometric force and mechanical power production of whole-muscle is not the relative distribution of the MHC isoforms, but rather, the respective anatomical cross-sectional area and total muscle mass that is composed of MHC II muscle. Our estimate of the total thigh lean mass composed of MHC II compared to MHC I revealed a 47% lower MHC II lean mass in old compared to young men with no differences in MHC I lean mass (Fig. 1). Most importantly, the lower MHC II lean mass in old adults described 74% of the variance in knee extensor power and 62% of the variance in isometric torque output with age. Notably, the estimated 47% lower MHC II lean mass was in close agreement with the ~55% smaller cross-sectional area observed in the isolated MHC IIa and IIa/IIx fibres from old compared to young adults. These findings suggest that the primary mechanism for the loss in muscle strength

and power with age is a selective atrophy of fast MHC II fibres. Whether the same mechanism is responsible for the age-related decrements in muscle strength and power in mobility impaired older adults or in old women remains unknown.

Paradoxically, despite a lower amount of muscle mass composed of the more fatigable MHC II fibres in old compared to young men, we observed an ∼2.7-fold increase in fatigability during the high-velocity exercise with age (Fig. **2**). Because the voluntary activation and vastus lateralis M-wave immediately following the fatiguing exercise did not change compared to baseline for either the old or young men, the increased age-related fatigability could not be attributed to either impaired neural drive or altered neuromuscular propagation. By contrast, 79% of the variance in the reductions in power during the fatiguing exercise was explained by the reduction in the rate of torque development of the involuntary electrically-evoked twitch (Fig. **2**). Although the specific cellular mechanisms cannot be identified by the electrically-evoked twitch, the strong correlation between the changes in the twitch properties and the reductions in power suggest that the age-related increase in fatigability during dynamic exercise is determined primarily by mechanisms that disrupt contractile function within the muscle.

P_i and H^+ inhibit cross-bridge function and are important mediators of muscle fatigue in humans

To test whether cross-bridge mechanisms could explain the age-related increase in fatigability, we exposed muscle fibres from the vastus lateralis of young and old men to conditions mimicking quiescent human muscle (pH 7.0 + 4 mM P_i) and severe fatigue (pH 6.2 + 30 mM P_i) at 15 and 30°C. We selected the severe fatigue condition because (i) human skeletal muscle can reach this level of metabolite accumulation during high-intensity volitional contractions (Taylor *et al*. **1986**; Wilson *et al*. **1988**; Cady *et al*. **1989**); (ii) we could more directly compare our data from human fibres with studies on rat and rabbit fibres (Karatzaferi *et al*. **2008**; Nelson *et al*. **2014**); and (iii) we anticipated that the age-differences in the sensitivity of the contractile proteins to these ions, if present, would be most obvious in a severe fatigue condition. At 15°C, we found that the fatigue-mimicking condition caused marked reductions in P_o, V_o and V_{max}, k_{tr}, and peak power of fibres from young and old men, and that the effect was greater in MHC II compared to MHC I fibres for V_o, k_{tr} and peak power, but not for P_o or V_{max}. As expected, increasing the temperature to 30°C increased all of the contractile parameters for the MHC I fibres. However, although the increase in temperature reduced the effect of the fatigue-mimicking condition on P_o by ∼50% (Fig. **3**), it had little-to-no effect on V_o, V_{max} and peak power, and exacerbated the effect on k_{tr} (Fig. **4**). In contrast to our hypothesis, we found no evidence in any of the contractile parameters that fibres from old adults were more sensitive to the depressive effects of H^+ and P_i compared to fibres from young adults. It should be noted, however, that these data were obtained in saturating Ca^{2+} conditions and that fatigue during high-intensity contractions probably also involves a decrease in myoplasmic free Ca^{2+} (Lee *et al*. **1991**; Allen *et al*. **2011**).

Our observation of a 37% lower P_o in the fatigue-mimicking condition compared to the ∼0 mM P_i control condition in MHC I fibres at 30°C was similar to the 36% decrease observed in slow fibres from rats studied under the same conditions (Nelson *et al*. **2014**). These findings suggest that, at least for MHC I fibres, the combined effects of H^+ and P_i on P_o are similar across mammalian species. However, when we compared the P_o of the fatigue-mimicking condition with the 4 mM P_i control condition, which is more representative of quiescent human skeletal muscle (Kemp *et al*. **2007**), the decrement in P_o was reduced to ∼21% (Fig. **3**). This finding suggests that other factors such as the P_i- and H^+-induced decreases in Ca^{2+} sensitivity (Palmer &

Kentish, **1994**; Parsons *et al.* **1997**; Debold *et al.* **2006**; Nelson & Fitts, **2014**) and/or decreases in myoplasmic free Ca^{2+} (Allen *et al.* **2011**) probably play an important role in the fatigue-induced reductions in P_o *in vivo*. In addition, the relatively large decrease in P_o when the [P_i] was increased from ~0 to 4 mM is consistent with other studies showing a hyperbolic relationship between the concentration of P_i and P_o (Fryer *et al.* **1995**; Wang & Kawai, **1997**; Coupland *et al.* **2001**; Tesi *et al.* **2002**; Pathare *et al.* **2005**). Importantly, because slow MHC I fibres are more sensitive to P_i at low concentrations compared to fast MHC II fibres (Fig. **3**) (Fryer *et al.* **1995**; Wang & Kawai, **1997**), the fibre type differences in the size-specific P_o (kN m^{-2}) were much greater at the more physiological [P_i] of 4 compared to ~0 mM.

As expected, increasing the [P_i] from ~0 to 4 mM increased the k_{tr} of both MHC I and MHC II fibres from young and old adults (Fig. **4**). This observation is consistent with the hypothesis that P_i decreases P_o by dissociating myosin from actin early in the low- to high-force transition of the cross-bridge cycle, resulting in a decreased number of high-force cross-bridges and an increased k_{tr} (Debold *et al.* **2016**). However, when H^+ (pH 6.2) was added with P_i (30 mM) in the condition mimicking fatigue, k_{tr} was reduced in both fibre types at 15°C, and the effect was exacerbated in MHC I fibres when the temperature was increased to 30°C (Fig. **4**). This novel finding supports the hypothesis that H^+ inhibits the forward rate constant of the low- to high-force transition of the cross-bridge cycle, and that previous studies underestimated this effect by using the ~0 mM P_i control condition (Metzger & Moss, **1990b**; Nelson *et al.* **2014**). The explanation for the increased effect at higher temperatures is unclear, but may be partly explained by a greater inhibition of the forward rate constant by H^+ at 30°C.

Interestingly, we observed no age differences in k_{tr} for the MHC I or II fibres from old compared to young adults (Fig. **4**). This is contrast to our hypothesis that was based on the lower k_{tr} reported in 'slow type' fibres in a group of old compared to young men (Power *et al.* **2016**). To our knowledge, this is the only other study to test the effect of age on the low- to high-force transition of the cross-bridge cycle by measuring k_{tr}. The explanation for the discrepancies between the present study and the study by **Power *et al.* (2016)** is unclear but may be the result of several factors, which include: (i) the study by **Power *et al.* (2016)** binned the 'slow type' fibres based on V_o, whereas we identified the MHC composition of the fibres with SDS-PAGE; (ii) the temperature of the experiments differed between the studies, with the present study performed at 15 and 30°C, and the study by **Power *et al.* (2016)** performed at 10°C; and (iii) the resting sarcomere spacing in the present study was set to 2.5 μm with direct measurements from an eyepiece micrometer, whereas **Power *et al.* (2016)** set the sarcomere spacing to ~2.8 μm using a fast Fourier transform analysis. It is also notable that the 'slow type' fibres from the old men studied by **Power *et al.* (2016)** had a lower V_o and size-specific P_o compared to the young men, whereas no age differences in any of the contractile parameters were observed in the present study.

Although increasing the [P_i] from ~0 to 4 mM had marked effects on P_o and k_{tr}, it had no effect on the V_o of MHC I or II fibres from young and old adults (Fig. **5**). This finding is consistent with the results from rat fibres that showed P_i had no effect on shortening velocity (Debold *et al.* **2004**; Karatzaferi *et al.* **2008**). However, when H^+ (pH 6.2) was added with P_i (30 mM) in the condition mimicking fatigue, the shortening velocity (V_o and V_{max}) was inhibited in both fibre types at 15°C, and remained inhibited in MHC I fibres when the temperature was increased to 30°C (Figs **5**-**8**). The inhibition of shortening velocity on human fibres was generally in close agreement with studies on rat fibres using either the combined pH 6.2 + 30 mM P_i condition (Nelson *et al.* **2014**) or a pH 6.2 only condition (Knuth *et al.* **2006**), which suggests that H^+ is the primary ion that depresses velocity (Metzger & Moss, **1987**; Karatzaferi *et al.* **2008**). Although the mechanism by which H^+ slows shortening velocity has not been fully elucidated, the primary hypothesis is that acidosis slows the ADP-bound isomerization step and/or the release of ADP from myosin (Debold *et al.* **2016**). Importantly, increasing the temperature to 30°C

had little-to-no effect on the fatigue-induced reduction in shortening velocity for MHC I fibres (Fig. **5** and Table **4**).

Because the ability of muscle to generate power is essential for older adults to maintain daily function (Reid & Fielding, **2012**), the effects of H^+ and P_i on fibre power are more important than their effects on peak isometric force or the maximum shortening velocity alone. We observed that the fatigue-mimicking condition induced a 57% decrease in peak fibre power in fast MHC II fibres (Fig. **6**) and a 48% decrease in power for slow MHC I fibres (Fig. **7**). Although the fatigue-induced decrements in fibre power did not differ with age, the absolute power generated in the MHC II fibres from old adults may have reached a critically low level in the fatigue condition where maintaining balance and the necessary power for movement may be compromised. Independent of age, the fibre type dependence for the loss in power was a result of the increased curvature (i.e. decreased a/P_o) of the force–velocity relationship in the fatigue-mimicking condition for the fast fibres that was not observed in slow fibres (Tables **3** and **4**). Notably, the fibre-type differences that we observed in the H^+- and P_i-induced decrements in power were not observed under a similar fatigue-mimicking condition in rat fibres (Nelson *et al*. **2014**). The discrepancies between studies may be due to differences in the contractile kinetics between mammalian species, or perhaps because a more physiological $[P_i]$ of 4 mM was used in the present study compared to the ∼0 mM P_i condition used by **Nelson *et al*. (2014)**.

Increasing the temperature from 15 to 30°C resulted in more than a 30-fold increase in peak fibre power and more than a 7-fold increase in the curvature constant (a/P_o) of the force–velocity relationship for slow MHC I fibres. The increase in the curvature constant to 0.22 in 30°C (Table **4**) is the same as the force–velocity curvature constant reported for the human adductor pollicis muscle *in vivo* (De Ruiter *et al*. **2000**; Jones *et al*. **2006**; Jones, **2010**), a muscle composed of ∼80% MHC I fibres (Round *et al*. **1984**). Additionally, the fatigue-mimicking condition caused a 43% decrease in peak fibre power, which was greater than could be attributed to the combined 21% and 11% decreases in P_o and V_{max}, respectively (Fig. **8**). The larger decrement in fibre power was explained by the 29% decrease in a/P_o (i.e. an increase in the curvature of the force–velocity relationship). These findings are strikingly similar to the changes observed in the force–velocity relationship of the fatigued human adductor pollicis muscle *in vivo* (De Ruiter *et al*. **2000**; Jones *et al*. **2006**; Jones, **2010**) and provide evidence that H^+ and P_i are important mediators of muscle fatigue in humans by directly inhibiting cross-bridge function.

Concluding remarks

Both neural drive and single fibre contractile function were well-preserved in old compared to young men, providing little evidence for an age-related decrease in 'muscle quality'. Instead, we found that the age-related loss in whole-muscle strength and power was strongly associated with the selective atrophy of fast MHC II fibres. Thus, we propose that caution is warranted when interpreting lower size-specific strength and power as evidence for a decrease in 'muscle quality'. We also provide the first evidence to confirm the findings from non-human studies that elevated levels of H^+ and P_i act synergistically to depress cross-bridge function and conclude that these ions are important mediators of muscle fatigue in humans.

References

Allen DG, Clugston E, Petersen Y, Roder IV, Chapman B & Rudolf R. (2011). Interactions between intracellular calcium and phosphate in intact mouse muscle during fatigue. *J Appl Physiol (1985)* **111**, 358– 366.

Baudry S, Klass M, Pasquet B & Duchateau J. (2007). Age-related fatigability of the ankle dorsiflexor muscles during concentric and eccentric contractions. *Eur J Appl Physiol* **100**, 515– 525.

Bergstrom J. (1962). Muscle electrolytes in man. *Scand J Clin Lab Invest* **68**, 1– 110.

Brenner B & Eisenberg E. (1986). Rate of force generation in muscle: correlation with actomyosin ATPase activity in solution. *Proc Natl Acad Sci U S A* **83**, 3542– 3546.

Cady EB, Jones DA, Lynn J & Newham DJ. (1989). Changes in force and intracellular metabolites during fatigue of human skeletal muscle. *J Physiol* **418**, 311– 325.

Callahan DM & Kent-Braun JA. (2011). Effect of old age on human skeletal muscle force-velocity and fatigue properties. *J Appl Physiol (1985)* **111**, 1345– 1352.

Caremani M, Melli L, Dolfi M, Lombardi V & Linari M. (2013). The working stroke of the myosin II motor in muscle is not tightly coupled to release of orthophosphate from its active site. *J Physiol* **591**, 5187– 5205.

Chase PB & Kushmerick MJ. (1988). Effects of pH on contraction of rabbit fast and slow skeletal muscle fibers. *Biophys J* **53**, 935– 946.

Cooke R, Franks K, Luciani GB & Pate E. (1988). The inhibition of rabbit skeletal muscle contraction by hydrogen ions and phosphate. *J Physiol* **395**, 77– 97.

Coupland ME, Puchert E & Ranatunga KW. (2001). Temperature dependence of active tension in mammalian (rabbit psoas) muscle fibres: effect of inorganic phosphate. *J Physiol* **536**, 879– 891.

D'Antona G, Pellegrino MA, Adami R, Rossi R, Carlizzi CN, Canepari M, Saltin B & Bottinelli R. (2003). The effect of ageing and immobilization on structure and function of human skeletal muscle fibres. *J Physiol* **552**, 499– 511.

Dalton BH, Power GA, Vandervoort AA & Rice CL. (2010). Power loss is greater in old men than young men during fast plantar flexion contractions. *J Appl Physiol (1985)* **109**, 1441– 1447.

Dalton BH, Power GA, Vandervoort AA & Rice CL. (2012). The age-related slowing of voluntary shortening velocity exacerbates power loss during repeated fast knee extensions. *Exp Gerontol* **47**, 85– 92.

Dantzig JA, Goldman YE, Millar NC, Lacktis J & Homsher E. (1992). Reversal of the cross-bridge force-generating transition by photogeneration of phosphate in rabbit psoas muscle fibres. *J Physiol* **451**, 247– 278.

De Ruiter CJ, Didden WJ, Jones DA & Haan AD. (2000). The force-velocity relationship of human adductor pollicis muscle during stretch and the effects of fatigue. *J Physiol* **526 Pt 3**, 671– 681.

Debold EP, Dave H & Fitts RH. (2004). Fiber type and temperature dependence of inorganic phosphate: implications for fatigue. *Am J Physiol Cell Physiol* **287**, C673– C681.

Debold EP, Fitts RH, Sundberg CW & Nosek TM. (2016). Muscle fatigue from the perspective of a single crossbridge. *Med Sci Sports Exerc* **48**, 2270– 2280.

Debold EP, Romatowski J & Fitts RH. (2006). The depressive effect of P_i on the force-pCa relationship in skinned single muscle fibers is temperature dependent. *Am J Physiol Cell Physiol* **290**, C1041– C1050.

Doherty TJ. (2003). Invited review: aging and sarcopenia. *J Appl Physiol (1985)* **95**, 1717– 1727.

Edman KA. (1979). The velocity of unloaded shortening and its relation to sarcomere length and isometric force in vertebrate muscle fibres. *J Physiol* **291**, 143– 159.

Fabiato A. (1988). Computer programs for calculating total from specified free or free from specified total ionic concentrations in aqueous solutions containing multiple metals and ligands. *Methods Enzymol* **157**, 378– 417.

Fabiato A & Fabiato F. (1979). Calculator programs for computing the composition of the solutions containing multiple metals and ligands used for experiments in skinned muscle cells. *J Physiol (Paris)* **75**, 463– 505.

Fitts RH. (1994). Cellular mechanisms of muscle fatigue. *Physiol Rev* **74**, 49– 94.

Fitts RH. (2008). The cross-bridge cycle and skeletal muscle fatigue. *J Appl Physiol (1985)* **104**, 551– 558.

Fitts RH. (2016). The role of acidosis in fatigue: pro perspective. *Med Sci Sports Exerc* **48**, 2335– 2338.

Frontera WR, Reid KF, Phillips EM, Krivickas LS, Hughes VA, Roubenoff R & Fielding RA. (2008). Muscle fiber size and function in elderly humans: a longitudinal study. *J Appl Physiol (1985)* **105**, 637– 642.

Frontera WR, Suh D, Krivickas LS, Hughes VA, Goldstein R & Roubenoff R. (2000). Skeletal muscle fiber quality in older men and women. *Am J Physiol Cell Physiol* **279**, C611– C618.

Fryer MW, Owen VJ, Lamb GD & Stephenson DG. (1995). Effects of creatine phosphate and P_i on Ca^{2+} movements and tension development in rat skinned skeletal muscle fibres. *J Physiol* **482**, 123– 140.

Fuglevand AJ, Zackowski KM, Huey KA & Enoka RM. (1993). Impairment of neuromuscular propagation during human fatiguing contractions at submaximal forces. *J Physiol* **460**, 549– 572.

Giulian GG, Moss RL & Greaser M. (1983). Improved methodology for analysis and quantitation of proteins on one-dimensional silver-stained slab gels. *Anal Biochem* **129**, 277– 287.

Godt RE & Nosek TM. (1989). Changes of intracellular milieu with fatigue or hypoxia depress contraction of skinned rabbit skeletal and cardiac muscle. *J Physiol* **412**, 155– 180.

Grosicki GJ, Standley RA, Murach KA, Raue U, Minchev K, Coen PM, Newman AB, Cummings S, Harris T, Kritchevsky S, Goodpaster BH & Trappe S. (2016). Improved single muscle fiber quality in the oldest-old. *J Appl Physiol (1985)* **121**, 878– 884.

Hart TL, Swartz AM, Cashin SE & Strath SJ. (2011). How many days of monitoring predict physical activity and sedentary behaviour in older adults? *Int J Behav Nutr Phys Act* **8**, 62.

Hassanlouei H, Sundberg CW, Smith AE, Kuplic A & Hunter SK. (2017). Physical activity modulates corticospinal excitability of the lower limb in young and old adults. *J Appl Physiol (1985)* **123**, 364– 374.

Hepple RT & Rice CL. (2016). Innervation and neuromuscular control in ageing skeletal muscle. *J Physiol* **594**, 1965– 1978.

Hill AV. (1938). The heat of shortening and the dynamic constants of muscle. *Proc R Soc Lond B Biol Sci* **126**, 136– 195.

Hunter SK. (2017). Performance Fatigability: mechanisms and Task Specificity. *Cold Spring Harb Perspect Med*.

Hunter SK, Butler JE, Todd G, Gandevia SC & Taylor JL. (2006). Supraspinal fatigue does not explain the sex difference in muscle fatigue of maximal contractions. *J Appl Physiol (1985)* **101**, 1036– 1044.

Hunter SK, Pereira HM & Keenan KG. (2016). The aging neuromuscular system and motor performance. *J Appl Physiol (1985)* **121**, 982– 995.

Jones DA. (2010). Changes in the force-velocity relationship of fatigued muscle: implications for power production and possible causes. *J Physiol* **588**, 2977– 2986.

Jones DA, de Ruiter CJ & de Haan A. (2006). Change in contractile properties of human muscle in relationship to the loss of power and slowing of relaxation seen with fatigue. *J Physiol* **576**, 913– 922.

Karatzaferi C, Franks-Skiba K & Cooke R. (2008). Inhibition of shortening velocity of skinned skeletal muscle fibers in conditions that mimic fatigue. *Am J Physiol Regul Integr Comp Physiol* **294**, R948– R955.

Kemp GJ, Meyerspeer M & Moser E. (2007). Absolute quantification of phosphorus metabolite concentrations in human muscle in vivo by ^{31}P MRS: a quantitative review. *NMR Biomed* **20**, 555– 565.

Kent-Braun JA, Fitts RH & Christie A. (2012). Skeletal Muscle Fatigue. *Compr Physiol* **2**, 997– 1044.

Kent-Braun JA, Ng AV & Young K. (2000). Skeletal muscle contractile and noncontractile components in young and older women and men. *J Appl Physiol (1985)* **88**, 662– 668.

Klass M, Baudry S & Duchateau J. (2007). Voluntary activation during maximal contraction with advancing age: a brief review. *Eur J Appl Physiol* **100**, 543– 551.

Knuth ST, Dave H, Peters JR & Fitts RH. (2006). Low cell pH depresses peak power in rat skeletal muscle fibres at both 30°C and 15°C: implications for muscle fatigue. *J Physiol* **575**, 887– 899.

Korhonen MT, Cristea A, Alen M, Hakkinen K, Sipila S, Mero A, Viitasalo JT, Larsson L & Suominen H. (2006). Aging, muscle fiber type, and contractile function in sprint-trained athletes. *J Appl Physiol (1985)* **101**, 906– 917.

Lamboley CR, Wyckelsma VL, Dutka TL, McKenna MJ, Murphy RM & Lamb GD. (2015). Contractile properties and sarcoplasmic reticulum calcium content in type I and type II skeletal muscle fibres in active aged humans. *J Physiol* **593**, 2499– 2514.

Lamboley CR, Wyckelsma VL, McKenna MJ, Murphy RM & Lamb GD. (2016). Ca^{2+} leakage out of the sarcoplasmic reticulum is increased in type I skeletal muscle fibres in aged humans. *J Physiol* **594**, 469– 481.

Larsson L, Li X & Frontera WR. (1997). Effects of aging on shortening velocity and myosin isoform composition in single human skeletal muscle cells. *Am J Physiol Cell Physiol* **272**, C638– C649.

Lee JA, Westerblad H & Allen DG. (1991). Changes in tetanic and resting $[Ca^{2+}]_i$ during fatigue and recovery of single muscle fibres from *Xenopus laevis*. *J Physiol* **433**, 307– 326.

Lexell J. (1995). Human aging, muscle mass, and fiber type composition. *J Gerontol A Biol Sci Med Sci* **50**, 11– 16.

Linari M, Caremani M & Lombardi V. (2010). A kinetic model that explains the effect of inorganic phosphate on the mechanics and energetics of isometric contraction of fast skeletal muscle. *Proc Biol Sci* **277**, 19– 27.

Maden-Wilkinson TM, Degens H, Jones DA & McPhee JS. (2013). Comparison of MRI and DXA to measure muscle size and age-related atrophy in thigh muscles. *J Musculoskelet Neuronal Interact* **13**, 320– 328.

McNeil CJ & Rice CL. (2007). Fatigability is increased with age during velocity-dependent contractions of the dorsiflexors. *J Gerontol A Biol Sci Med Sci* **62**, 624– 629.

Metzger JM, Greaser ML & Moss RL. (1989). Variations in cross-bridge attachment rate and tension with phosphorylation of myosin in mammalian skinned skeletal muscle fibers. Implications for twitch potentiation in intact muscle. *J Gen Physiol* **93**, 855– 883.

Metzger JM & Moss RL. (1987). Greater hydrogen ion-induced depression of tension and velocity in skinned single fibres of rat fast than slow muscles. *J Physiol* **393**, 727– 742.

Metzger JM & Moss RL. (1990a). Calcium-sensitive cross-bridge transitions in mammalian fast and slow skeletal muscle fibers. *Science* **247**, 1088– 1090.

Metzger JM & Moss RL. (1990b). pH modulation of the kinetics of a Ca^{2+}-sensitive cross-bridge state transition in mammalian single skeletal muscle fibres. *J Physiol* **428**, 751– 764.

Miller MS, Bedrin NG, Ades PA, Palmer BM & Toth MJ. (2015). Molecular determinants of force production in human skeletal muscle fibers: effects of myosin isoform expression and cross-sectional area. *Am J Physiol Cell Physiol* **308**, C473– C484.

Miller MS, Bedrin NG, Callahan DM, Previs MJ, Jennings ME, 2nd, Ades PA, Maughan DW, Palmer BM & Toth MJ. (2013). Age-related slowing of myosin actin cross-bridge kinetics is sex specific and predicts decrements in whole skeletal muscle performance in humans. *J Appl Physiol (1985)* **115**, 1004– 1014.

Miller MS & Toth MJ. (2013). Myofilament protein alterations promote physical disability in aging and disease. *Exerc Sport Sci Rev* **41**, 93– 99.

Moss RL. (1979). Sarcomere length-tension relations of frog skinned muscle fibres during calcium activation at short lengths. *J Physiol* **292**, 177– 192.

Nelson CR, Debold EP & Fitts RH. (2014). Phosphate and acidosis act synergistically to depress peak power in rat muscle fibers. *Am J Physiol Cell Physiol* **307**, C939– C950.

Nelson CR & Fitts RH. (2014). Effects of low cell pH and elevated inorganic phosphate on the pCa-force relationship in single muscle fibers at near-physiological temperatures. *Am J Physiol Cell Physiol* **306**, C670– C678.

Palmer S & Kentish JC. (1994). The role of troponin C in modulating the Ca^{2+} sensitivity of mammalian skinned cardiac and skeletal muscle fibres. *J Physiol* **480**, 45– 60.

Parsons B, Szczesna D, Zhao J, Van Slooten G, Kerrick WG, Putkey JA & Potter JD. (1997). The effect of pH on the Ca^{2+} affinity of the Ca^{2+} regulatory sites of skeletal and cardiac troponin C in skinned muscle fibres. *J Muscle Res Cell Motil* **18**, 599– 609.

Pate E & Cooke R. (1989). Addition of phosphate to active muscle fibers probes actomyosin states within the powerstroke. *Pflugers Arch* **414**, 73– 81.

Pathare N, Walter GA, Stevens JE, Yang Z, Okerke E, Gibbs JD, Esterhai JL, Scarborough MT, Gibbs CP, Sweeney HL & Vandenborne K. (2005). Changes in inorganic phosphate and force production in human skeletal muscle after cast immobilization. *J Appl Physiol (1985)* **98**, 307– 314.

Power GA, Minozzo FC, Spendiff S, Filion ME, Konokhova Y, Purves-Smith MF, Pion C, Aubertin-Leheudre M, Morais JA, Herzog W, Hepple RT, Taivassalo T & Rassier DE. (2016). Reduction in single muscle fiber rate of force development with aging is not attenuated in world class older masters athletes. *Am J Physiol Cell Physiol* **310**, C318– C327.

Reid KF & Fielding RA. (2012). Skeletal muscle power: a critical determinant of physical functioning in older adults. *Exerc Sport Sci Rev* **40**, 4– 12.

Round JM, Jones DA, Chapman SJ, Edwards RH, Ward PS & Fodden DL. (1984). The anatomy and fibre type composition of the human adductor pollicis in relation to its contractile properties. *J Neurol Sci* **66**, 263– 272.

Rozand V, Senefeld JW, Hassanlouei H & Hunter SK. (2017). Voluntary activation and variability during maximal dynamic contractions with aging. *Eur J Appl Physiol* **117**, 2493– 2507.

Russ DW, Gregg-Cornell K, Conaway MJ & Clark BC. (2012). Evolving concepts on the age-related changes in "muscle quality". *J Cachexia Sarcopenia Muscle* **3**, 95– 109.

Sidhu SK, Bentley DJ & Carroll TJ. (2009). Cortical voluntary activation of the human knee extensors can be reliably estimated using transcranial magnetic stimulation. *Muscle Nerve* **39**, 186– 196.

Slivka D, Raue U, Hollon C, Minchev K & Trappe S. (2008). Single muscle fiber adaptations to resistance training in old (>80 yr) men: evidence for limited skeletal muscle plasticity. *Am J Physiol Regul Integr Comp Physiol* **295**, R273– R280.

Sundberg CW, Kuplic A, Hassanlouei H & Hunter SK. (2018). Mechanisms for the age-related increase in fatigability of the knee extensors in old and very old adults. *J Appl Physiol (1985)* **125**, 146– 158.

Taylor DJ, Styles P, Matthews PM, Arnold DA, Gadian DG, Bore P & Radda GK. (1986). Energetics of human muscle: exercise-induced ATP depletion. *Magn Reson Med* **3**, 44– 54.

Tesi C, Colomo F, Piroddi N & Poggesi C. (2002). Characterization of the cross-bridge force-generating step using inorganic phosphate and BDM in myofibrils from rabbit skeletal muscles. *J Physiol* **541**, 187– 199.

Todd G, Taylor JL & Gandevia SC. (2003). Measurement of voluntary activation of fresh and fatigued human muscles using transcranial magnetic stimulation. *J Physiol* **551**, 661– 671.

Trappe S, Gallagher P, Harber M, Carrithers J, Fluckey J & Trappe T. (2003). Single muscle fibre contractile properties in young and old men and women. *J Physiol* **552**, 47– 58.

Venturelli M, Saggin P, Muti E, Naro F, Cancellara L, Toniolo L, Tarperi C, Calabria E, Richardson RS, Reggiani C & Schena F. (2015). In vivo and in vitro evidence that intrinsic upper- and lower-limb skeletal muscle function is unaffected by ageing and disuse in oldest-old humans. *Acta Physiol (Oxf)* **215**, 58– 71.

Wahr PA, Cantor HC & Metzger JM. (1997). Nucleotide-dependent contractile properties of Ca^{2+}-activated fast and slow skeletal muscle fibers. *Biophys J* **72**, 822– 834.

Wang G & Kawai M. (1997). Force generation and phosphate release steps in skinned rabbit soleus slow-twitch muscle fibers. *Biophys J* **73**, 878– 894.

Westerblad H. (2016). Acidosis is not a significant cause of skeletal muscle fatigue. *Med Sci Sports Exerc* **48**, 2339– 2342.

Widrick JJ, Trappe SW, Costill DL & Fitts RH. (1996). Force-velocity and force–power properties of single muscle fibers from elite master runners and sedentary men. *Am J Physiol Cell Physiol* **271**, C676– C683.

Wilson JR, McCully KK, Mancini DM, Boden B & Chance B. (1988). Relationship of muscular fatigue to pH and diprotonated P_i in humans: a ^{31}P-NMR study. *J Appl Physiol (1985)* **64**, 2333– 2339.

Additional information

Competing interests

The authors declare that they have no competing interests.

Author contributions

CWS and RHF conceived and designed the experiments. CWS, SKH, SWT, CSS and RHF collected, analyzed and interpreted the data. CWS, SKH and RHF were involved in drafting the article or revising it critically for important intellectual content. All authors approved the final version of the manuscript submitted for publication and agree to be accountable for all aspects of the work. All persons designated as authors qualify for authorship, and all those who qualify for authorship are listed.

Funding

Acknowledgements